People's Democratic Republic of Algeria
Ministry of Higher Education and Scientific Research
Farhet Abbas-Setif1 University
Faculty of Sciences
Department of Physics

Thesis Submitted for the Degree of Doctor 3rd Cycle LMD of Physics in Radiophysics and Biomedical Imaging

Title:

Evaluation of a treatment planning and dose control system in external radiotherapy by experimental thermoluminescence dosimetry

Presented by: **Bouacid Serine Sarra**

Board of Examiners:

- **Pr. Ahmed BOUCENNA**, University of Setif1, President
- **Pr. Fayçal KHARFI**, University of Setif1, Thesis Director
- **Pr. Djamel MAOUCHE**, University of Setif1, Examiner
- **Dr. Nabil OUNOUGHI**, University of Jijel, Examiner
- **Dr. Fouad BOULAKHSSAIM**, Fighting Against Cancer Centre of Setif, Invited Member

-Thesis defended on October 15th, 2019-

List of Tables

Chapter II: In-vivo Dosimetry and TL Dosimetry in External Beam Radiotherapy

Chapter IV: Comparison of measured and calculated doses in a Rando phantom with a realistic lung radiotherapy treatment plan including heterogeneities

List of Figures

Chapter I: External Radiation Therapy

Chapter II: In-vivo Dosimetry and TL Dosimetry in External Beam Radiotherapy

Chapter III: Heterogeneity Correction in External Radiotherapy

Chapter IV: Comparison of measured and calculated doses in a Rando phantom with a realistic lung radiotherapy treatment plan including heterogeneities

Dedication

This thesis is dedicated to

My Dad Abdelkrim, the first man I ever loved. Thank you for letting me be my own woman and for all the love and support you give me.

My Mom Fairouz, you're an inspiration! Your love, cares and sacrifices I'll hold dear in my heart.

My beloved husband Ahmed, Thank you for your love and encouragements

My nephew Kenzi, the little angel you are .I love you

My loving sisters Ismahene, Manar, and my brother Alla.

My grandmother Yamina who lays in heaven peacefully.

Acknowledgments

I am and will forever be deeply grateful to Pr. F. Kharfi whom without his invaluable guidance, infinite discussions and encouragement throughout the thesis project I would have been lost.

I would like to express my sincere appreciation to the president and members of my thesis examining committee, Pr. A. Boucenna, Pr. D. Maouche, Dr. N. Ounoughi and Dr. F. Boulakhssaim, for kindly agreeing to serve on my examining committee

Special thanks to the professional and dedicated faculty of sciences of the University Farhat Abbas-Setif1 for providing the foundation of knowledge necessary.

I am also grateful to the entire staff at Setif's Anti-Cancer Center especially the physicists, dosimetrists, and therapists for their guidance and contribution to my preparation for entering into the medical physics profession. Special thanks to Mr. K. Benkahila, medical physicist, and Dr. F. Boulakhssaim, clinician, for their invaluable help and assistance in the achievement of this thesis project.

Content

Chapter II: In-vivo Dosimetry and TL Dosimetry in External Beam Radiotherapy

Chapter III: Heterogeneity Correction in External Radiotherapy

Chapter IV: Comparison of measured and calculated doses in a Rando phantom with a realistic lung radiotherapy treatment plan including heterogeneities

Abstract:
This thesis project aims to examine the compatibly of the calculated doses by the anisotropic analytical algorithm (AAA) and measured doses by thermoluminescent dosimeters (TLD) and therefore to evaluate the Eclipse-Varian TPS performance used in radiotherapy. Thus, it was a question to check if the treatment plans validated during the calculation phase is valid by dose measurement according to the ICRU recommendations on dose delivery to the treated volume (PTV) reported in reports 50 and 62. In this work, dose measurements was performed to evaluate an external radiotherapy treatment plan and, particularly, to validate dose calculations for a lung lesion case. Doses were calculated by the Varian Eclipse treatment planning system using the AAA algorithm. The measurements were performed using TLD700 and a Rando anthropomorphic phantom. The comparison between calculated and measured doses shows compatibility except for a few points, due to the limitations in the heterogeneity correction used for the case studied here. The deviation between calculated and measured doses was about 6.5% for low (<0.5Gy) doses, and about 1% for higher doses (>0.5Gy).The deviation between calculated and measured doses were also found to be higher in proximity to heterogeneous tissue interfaces.
Keywords: Radiotherapy; Dose calculation; Treatment planning system (TPS); Thermoluminescent dosimeter (TLD); Heterogeneity correction.

ملخص:
يهدف هذا المشروع إلى دراسة التوافق بين الجرعات الاشعاعيه المحسوبة بواسطة خوارزمية التحليل متباين الخواص AAA و الجرعات المقاسه باستعمال مقاييس الجرعات الفلورحرارية TLD، وبالتالي تقييم أداء نظام تخطيط علاج (TPS) Eclipse-Varian. الاشكاليه المدروسه كانت تتمحور حول معرفة ما إذا كانت خطط المعالجة التي تم التحقق منها خلال مرحلة الحساب صالحة و ذالك من خلال قياس الجرعات وفقًا لتوصيات ICRU بشأن الجرعة الواجب إعطاؤها للحجم المراد معالجته PTV والواردة في التقريرين 50 و 62. في هذا العمل ، أجريت قياسات الجرعة لتقييم خطة العلاج الإشعاعي الخارجي، ولا سيما للتحقق من صحة حسابات الجرعة لحالة سرطان الرئة. تم حساب الجرعات بواسطة نظامTPS Varian-Eclipse باستخدام خوارزمية AAA. تم إجراء القياسات باستخدام مقاييس الجرعات الفلورحرارية TLD700 والشبح مجسم الشكل Rando . توضح المقارنة بين الجرعات المحسوبة والجرعات المقاسة توافقا باستثناء بضع نقاط و ذالك بسبب بعض نقاط الضعف في خوارزمية تصحيح عدم التجانس المستخدمة للحالة التي تمت دراستها. يبلغ الانحراف بين الجرعات المحسوبة و الجرعات المقاسة حوالي 6.5٪ للجرعات المنخفضة (<0.5 غراي) وحوالي 1٪ للجرعات الأعلى (> 0.5 غراي). كما وجد أن الانحراف بين الجرعات المحسوبة والجرعات المقاسة يكون كبير على مقربة من محيطات الأنسجة غير المتجانسة.
كلمات مفتاحيه: العلاج الإشعاعي؛ حساب الجرعة؛ نظام تخطيط العلاج (TPS) ؛ مقياس الجرعات الحراري (TLD) ؛ تصحيح عدم التجانس.

Résumé:
Ce projet de thèse vise à examiner la compatibilité entre les doses calculées par l'algorithme calcul dose par analyse anisotrope (AAA) et celles mesurées par les dosimètres thermoluminescents (TLD) et à évaluer les performances du TPS Eclipse-Varian utilisé en radiothérapie. Ainsi, il a été nécessaire de vérifier si les plans de traitement validés au cours de la phase de calcul sont valables par expérimentalement par une mesure de dose par des TLDs et ce, conformément aux recommandations de l'ICRU concernant la dose à délivrer au volume PTV rapportés dans les rapports 50 et 62. Dans ce travail, des mesures de la dose ont été effectuées pour évaluer le plan de traitement de radiothérapie externe et, en particulier, pour valider le calcul de doses pour un cas de lésion pulmonaire. Les doses ont été calculées à l'aide du système de planification de traitement Varian-Eclipse en utilisant l'algorithme AAA. Les mesures ont été effectuées à l'aide de TLD700 sur le fantôme anthropomorphique Rando. La comparaison entre les doses calculées et les doses mesurées montre une compatibilité dans la majorité des points considérés à l'exception de quelques points en raison des limitations de l'algorithme de correction d'hétérogénéité utilisé sur le TPS. L'écart entre les doses calculées et les doses mesurées est d'environ 6,5% pour les doses faibles (<0,5 Gy) et d'environ 1% pour les doses les plus élevées (> 0,5 Gy). L'écart entre les doses calculées et les doses mesurées est également plus élevé à proximité d'interfaces tissulaires hétérogènes.
Mots-clés : Radiothérapie ; calcul de doses ; Système de planification de traitement (TPS) ; Dosimètre à thermoluminescence (TLD) ; Correction d'hétérogénistes.

Introduction

It is well-known that photon beam radiotherapy requires dose calculation algorithms as well as practical in-vivo dosimetry audits for an effective patient treatment [1-3]. Thermoluminescence (TL) is currently considered as one of the most versatile techniques for quantitative radiation dosimetry [4-6]. Thermoluminescence dosimetry is a very powerful technique for in-vivo measurements because it has the advantage of being very sensitive even for a small irradiated volume, and it does not need any electric power supply. In case of external radiotherapy, it is quite difficult to perform any in-vivo dosimetry at a certain depth of a patient regardless of the dosimeter that may be used.

The objective of this thesis project is the experimental evaluation of the performance of the Eclipse Vairan Treatment planning system (TPS) used at the fighting against cancer medical centre (CLCC) of Setif. This evaluation is performed through indirect dosimetry at different depths using the LiF-thermoluminescent dosimeter (TLD700) and a Rando phantom. This dosimetry is performed by considering a realistic lung radiotherapy treatment plan including tissue heterogeneities. In particular, it was the aim to assess the ability of the anisotropic analytical algorithm (AAA) –with its relative heterogeneity correction– to predict doses for a case including tissue heterogeneities[7-8].This study aims to examine the compatibility between the AAA-calculated and TL-measured doses. It is also a question to check if the treatment plan validated during the calculation phase is valid by TL measurement according to the ICRU recommendations on dose delivery to the programmed tumour volume (PTV) reported in reports 50 and 62 [9-10]**.** In this context, ICRU recommends that the delivered doses to PTV must be within the interval of 95% to 107% of the prescribed dose. Since the prescribed dose is 2Gy per session, calculated or measured doses must be within the dose interval of [1.9Gy-2.14Gy].

This thesis is subdivided into four chapters. The first chapter presents the essential theory and practice of the external radiotherapy. The second chapter includes a description of the in-vivo and thermoluminescence dosimetry. The third chapter presents the essential theory of the available heterogeneity correction methods used in external radiotherapy. The last chapter is reserved to the presentation of the experimental work performed in the framework of this thesis project which deals with the evaluation of the used TPS by the comparison of measured and calculated doses in a Rando phantom with the consideration of a realistic lung radiotherapy treatment plan including heterogeneities.

CHAPTER I

Radiation Therapy

I. Radiation therapy

Radiation therapy often abbreviated RT, is therapy using ionizing radiation, generally as part of cancer treatment to control or kill malignant cells. Radiation therapy may be curative in a number of types of cancer if they are localized to one area of the body. It may also be used as part of adjuvant therapy, to prevent tumor recurrence after surgery to remove a primary malignant tumor (for example, early stages of breast cancer).

I.1Internal radiation therapy (Brachytherapy)

Brachytherapy is the term used to describe radiation treatment in which the radiation source is in contact with the tumor. It places radioactive sources directly inside the patient to kill cancer cells and shrink tumors and has the advantage of using a highly localized dose of radiation. This means that less radiation is delivered to surrounding tissue.This therapy contrasts with external beam radiotherapy, in which the radiation source is 80-100 cm away from the patient.

The type of radioactive material used (iodine, palladium, cesium or iridium) depends on the type of treatment. In all types, the radiation source is encapsulated. This means it is enclosed within a non-radioactive metallic capsule often referred to as a "seed." This helps prevent the material from moving to other parts of the patient's body

Brachytherapy may be temporary or permanent:

Temporary brachytherapy places radioactive material inside a catheter for a specific amount of time and then removes it. It is given at a low-dose rate (LDR) or high-dose rate (HDR).

Permanent brachytherapy is also called seed implantation. It puts radioactive seeds (about the size of a grain of rice) in or near the tumor permanently. After several months, the seeds lose their radioactivity.

I.2 External beam radiotherapy

External beam radiotherapy (EBRT) or external radiation therapy is one of the three principal modalities used in the treatment of cancer, the other two being surgery and chemotherapy. It involves giving high energy ionizing radiation from a machine located outside the body fig (I.1). It can treat large areas of the body, if necessary. The use of ionizing radiation relies heavily on modern technology and the collaborative efforts of several professionals (radiation

oncologist, medical physicists, dosimetrists ...). The machine typically used to create the radiation beam is called a linear accelerator or linac. Computers with special software are used to adjust the size and shape of the beam and to direct it to target the tumor while avoiding the healthy tissue that surrounds the cancer cells. External-beam radiation therapy does not make the patients radioactive [11].

External beam therapy is the most commonly used technique to treat cancer. Often, the goal is to eliminate a tumor or prevent a tumor from returning. The procedure may also be performed before or after surgery to remove a cancerous tumor, to reduce the tumor size before surgery, or to prevent the tumor from coming back after surgery. EBRT may also be used as a palliative treatment in patients with advanced stage cancer or cancer that has metastasized. In this case, the goal of therapy is to reduce a patient's symptoms rather than cure the cancer.

External beam therapy is used to treat the following diseases as well as many others:

- Breast Cancer.
- Lung Cancer.
- Colorectal (Bowel) Cancer.
- Esophageal Cancer.
- Head and Neck Cancer.
- Prostate Cancer.
- Brain Tumor.

Fig (I.1): External beam radiation therapy

I.3 Types of radiation used in external beam radiotherapy

Radiation used for cancer treatment is called ionizing radiation because it forms ions (electrically charged particles) in the cells of the tissues it passes through. It creates ions by removing electrons from atoms and molecules. This can kill cells or change genes so the cells stop growing [12].

Ionizing radiation can be sorted into two major types:

- **Photon radiation**

  High-energy photon beam is by far the most common form of radiation used for cancer treatment. It is the same type of radiation that is used in x-ray machines, and comes from a radioactive source such as cobalt, cesium, or a machine called a linear accelerator (linac) Photon beams of energy affect the cells along their path as they go through the body to get to the cancer, pass through the cancer, and then exit the body Fig (I.2).

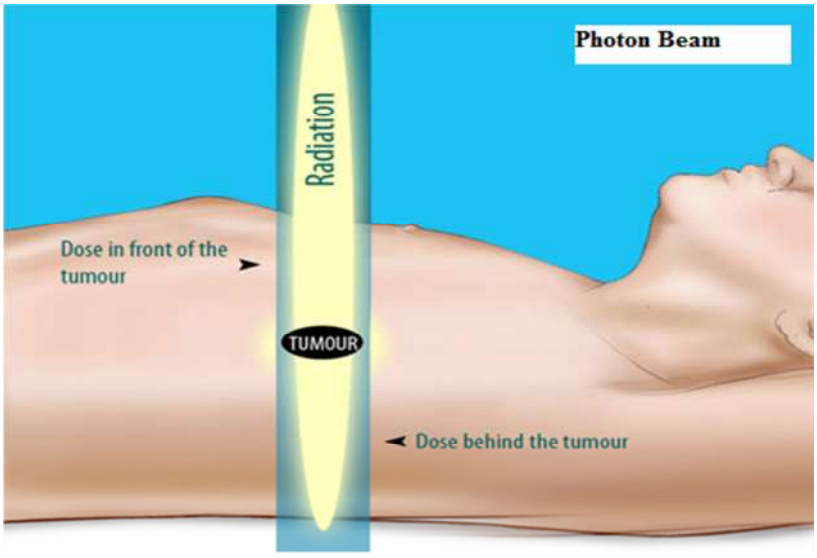

Fig (I.2): photon beam radiation

The photon beam used in therapy is mainly sorted into three major types:

- ❖ Superficial (30KeV to 100KeV): was used for treatment of small superficial skin tumors.
- ❖ Orthovoltage (100KeV to 300KeV): was used to treat superficial but thick tumors of the skin.
- ❖ Megavoltage (1MV to 25MV, like Cobalt and linac): used to treat deeply situated tumors

- **Particle radiation**

Electron beams or particle beams are also produced by a linear accelerator. Electrons are negatively charged parts of atoms. They have a low energy level and don't penetrate deeply into the body, so this type of radiation is used most often to treat the skin, as well as tumors and lymph nodes that are close to the surface of the body.

Proton beams are a form of particle beam radiation. Protons are positively charged parts of atoms. They release their energy only after traveling a certain distance and cause little damage to the tissues they pass through. This makes them very good at killing cells at the end of their path. So, proton beams are thought to be able to deliver more radiation to the cancer while doing less damage to nearby normal tissues Fig (I.3). Proton beam radiation therapy requires highly specialized equipment and is not widely available.

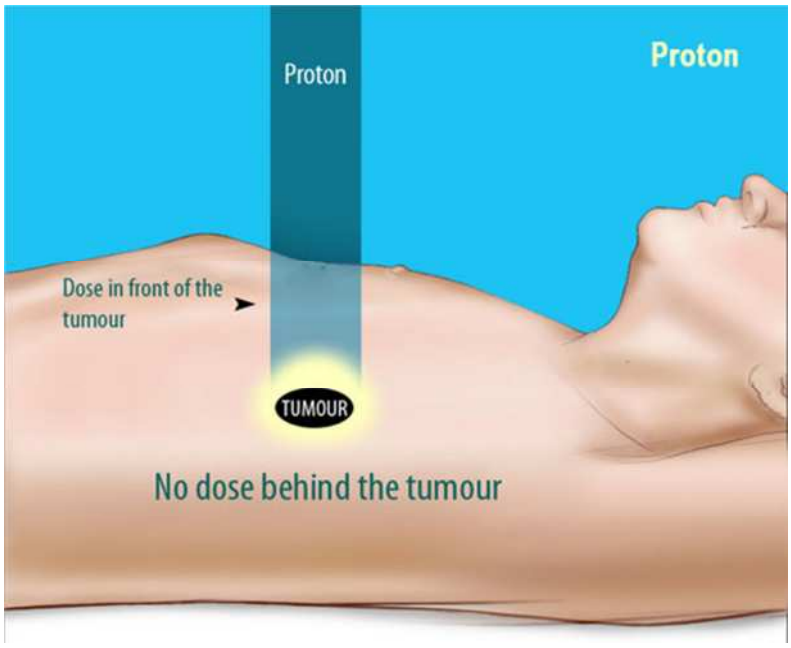

Fig (I.3): Proton beam radiation

The more energy, the more deeply the radiation can penetrate the tissues. The way each type of radiation behaves is important in planning radiation treatments. The radiation oncologist selects the type of radiation that's most suitable for each patient's cancer type and location.

I.4 Types of external-beam radiation therapy

I.4.1 Three-dimensional conformal radiation therapy (3D-CRT)

This technique uses imaging scan pictures and special computers to map the location of a tumor very precisely in 3 dimensions. The patient is fitted with a plastic mold or cast to keep the body part still during treatment. 3D conformal radiotherapy delivers radiation beams in multiple arcs at various angles fig (I.4). It uses collimators to shape each radiation beam to conform to the tumor volume .Careful aiming of the radiation beam may help reduce radiation damage to normal tissues and better fight the cancer by increasing the radiation dose to the tumor. A drawback of 3D-CRT is that it can be hard to see the full extent of some tumors on imaging tests, and any part not seen will not get treated with this therapy [13].

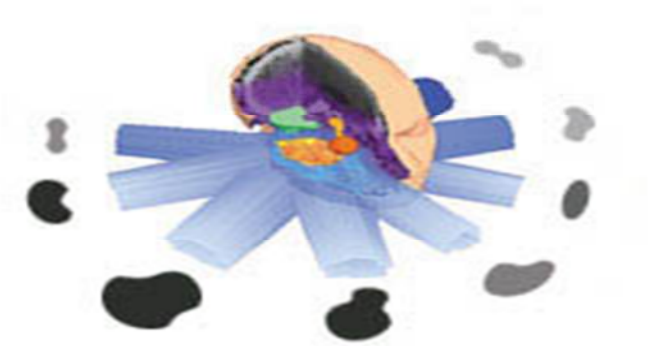

Fig (I.4):3D-Conformal radiation therapy

I.4.2 Conformal proton beam radiation therapy

Conformal proton beam radiation therapy is much like conformal therapy, but it uses proton beams instead of x-rays. Protons are parts of atoms that cause little damage to tissues they pass through but are very good at killing cells at the end of their path. This means that proton beam radiation may be able to deliver more radiation to the tumor while reducing side effects on normal tissues. Protons can only be put out by a special machine called a cyclotron or synchrotron. This machine costs a lot and requires expert staff. This is why proton beam therapy costs a lot and is only in a small number of radiation treatment centers. More studies are needed to find out if proton radiation gives better results in certain cancers than other types of radiation treatment [13].

I.4.3 Intensity modulated radiation therapy (IMRT)

This is an advanced form of external radiation therapy. As with 3D-CRT, computer programs are used to precisely map the tumor in 3 dimensions. But along with aiming photon beams from several directions, the intensity (strength) of the beams can be adjusted. This gives even

more control over the dose, decreasing the radiation reaching sensitive normal tissues while delivering higher doses to the tumor.

Because of its precision, it's even more important that a person remain in the right position and be perfectly still during treatment. A special cast or mold may be made to keep the body in place during treatment. Again, miscalculations in tumor size and exact location can mean missed areas will not get treated [13].

I.4.4 Intraoperative radiation therapy (IORT)

Intraoperative radiation therapy is external radiation given directly to the tumor or tumors during surgery fig (I.5). It may be used if the tumors can't be removed completely or if there's a high risk the cancer will come back in the same area. The surgeon finds the cancer while the patient is under anesthesia Normal tissues are moved out of the way and protected with special shields, so IORT lets the doctor give one large dose of radiation to the cancer and limit the effects on nearby tissues. IORT is usually given in a special operating room that has radiation-shielding walls.

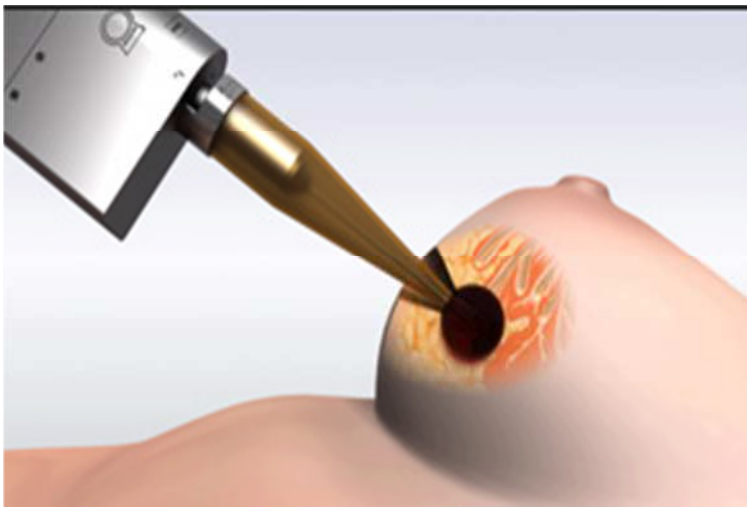

Fig (I.5): Intraoperative radiation therapy

I.5 Treatment planning in external beam radiation

The process of external beam therapy involves four major parts

1. Diagnosis

2. Simulation
3. Treatment Planning
4. Treatment Delivery and Quality assurance of the treatment

During the patients initial doctor's visit, doctors will recommend a biopsy or imaging study, such as an CT-scan or MRI, When choosing a diagnostic test(s), the doctor will consider the person's age and medical condition and the type of cancer suspected. Based on this analysis, once the patient is diagnosed with cancer other tests are required. After cancer is diagnosed, it is staged. Staging is a way of describing how advanced the cancer has become, including such criteria as how big it is and whether it has spread to neighboring tissues or more distantly to lymph nodes or other organs. The oncologist manages care and treatment and determines the proper dose of radiation for the particular treated cancer. The dose is divided into smaller doses called fractions. This process in external beam radiation therapy takes several days to complete. But it's a key part of successful radiation treatment. The radiation team will design a treatment for each patient individually. The treatment will give the strongest dose of radiation to the cancer while sparing normal tissue as much as possible.

The second part of treatment planning is called simulation. It's sometimes referred to as a "marking session." The patient will be asked to lie still on a table while the health care team works out the best treatment position and how to keep the patient in that position (tape, headrests, casts, body molds Fig(I.6), or foam pillows may be used). They will then mark the radiation field (also called the treatment port), which is the exact place on the body where the radiation will be aimed. The marks may be done with permanent markers or with tattoos that look like tiny freckles.

Fig (I.6): Head-chest mold used for patients positioning and immobilization in EBRT

The doctor may use imaging tests to check again the size of the tumor, figure out where it's most likely to have spread, outline normal tissues in the treatment area, take measurements, and plan the treatment. Photos may also be taken and are used to make the daily treatment set-up easier.

The area selected for treatment usually includes the whole tumor plus a small amount of normal tissue surrounding the tumor. The normal tissue is treated for two main reasons:

- To take into account body movement from breathing and normal movement of the organs within the body, this can change the location of a tumor between treatments.
- To reduce the likelihood of tumor recurrence from cancer cells that have spread to the normal tissue next to the tumor (called microscopic local spread).

Fig (I.7): Siemens CT-Scanner used for imaging tests

Through a complex process called dosimetry fig (I.8), treatment planning system is used to find out how much radiation the nearby normal structures would be exposed to if the prescribed dose were delivered to the cancer. The doctor and dosimetrist will work together to decide on the amount of radiation the patient needs to get and the best ways to aim it at the cancer. They base this on the size of the tumor, how sensitive the tumor is to radiation, and how well the normal tissue in the area can withstand the radiation.

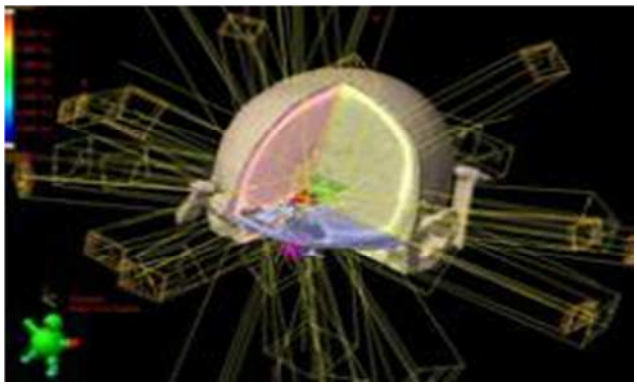

Fig (I.8) Dosimetry in radiation therapy

After the simulation and planning have been completed, the treatment can begin. Before each treatment session, the patient may be asked to change into a gown. The radiation therapist brings the patient into the treatment room and places him/her on the treatment couch of the linear accelerator in exactly the same position that was used for simulation using the same immobilization devices. The therapist carefully positions the patient using the alignment lasers and the marks that had been placed on the patient during simulation. Some form of imaging is often used prior to the treatment delivery to verify the accuracy of the patient setup. Some of the types of imaging that can be used include x-rays and cone beam CT. The therapist goes outside the room and turns on the linear accelerator from outside Fig (I.9). Beams from one or more directions may be used and the beam may be on for as long as several minutes for each field.

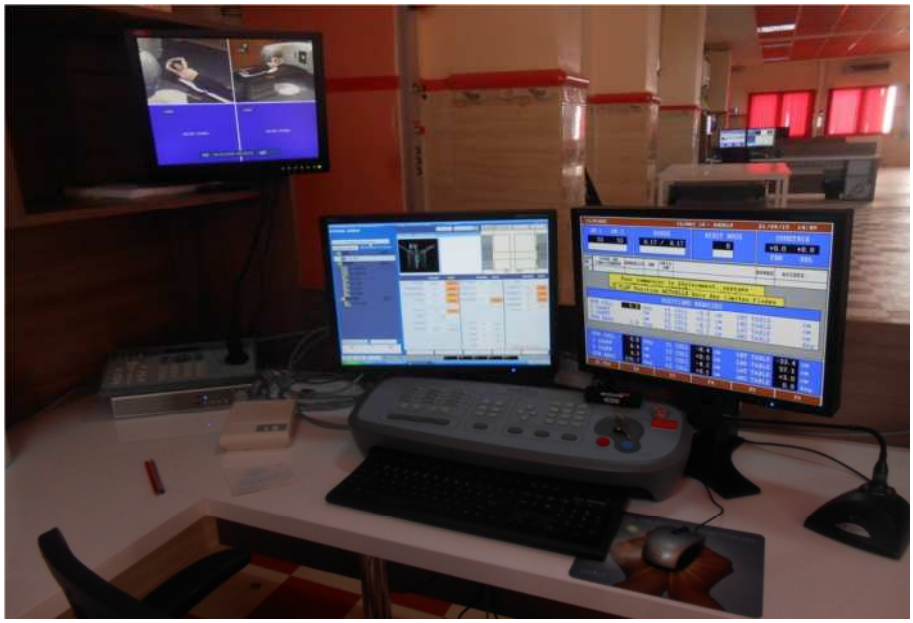

Fig (I.9): Linac control panel

The treatment process can take one hour or less each day and most of the time is often spent on positioning and imaging the patient. The actual treatment may last only several minutes. The duration of a patient's treatment depends on the method of treatment delivery, such as IMRT or 3D CRT, and the dose given. The length of each treatment will usually be the same from day to day [14].

Once treatment is complete, patients are asked to return for follow-up visits. During these appointments, patients will undergo evaluation, including imaging exams or blood tests, to determine if their cancer has been eliminated or if additional treatment is required. Even if the

cancer has been cured, patients can expect to continue periodic visits to follow-up with their doctor. The whole process of treatment is described by the scheme in fig (I.10).

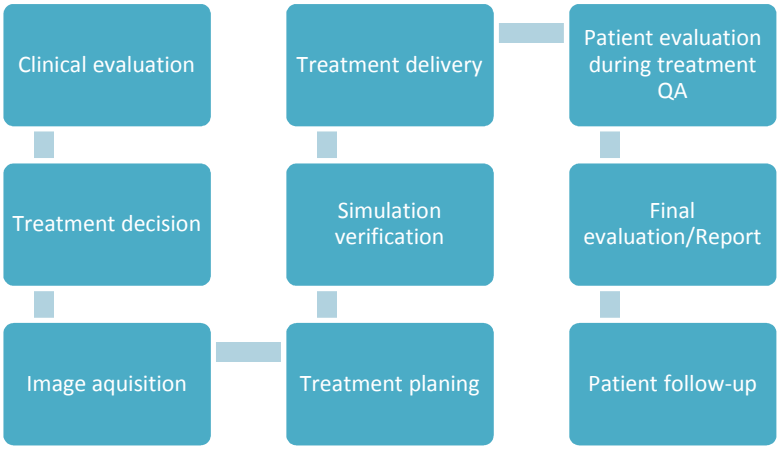

Fig (I.10): Process of treatment in external radiation therapy.

I.6 Clinical treatment planning in external photon beam radiotherapy

External photon beam radiotherapy is usually carried out with more than one radiation beam in order to achieve a uniform dose distribution inside the target volume and an as low as possible a dose in healthy tissues surrounding the target. ICRU Report No. 50 recommends a target dose uniformity within +7% and –5% of the dose delivered to a well-defined prescription point within the target. External radiotherapy is carried out with a variety of beam energies and field sizes under one of two set-up conventions:

- source to surface distance set-up (SSD) : the distance from the source to the surface of the patient is kept constant for all beams
- source to axis distance (SAD) : the centre of the target volume is placed at the machine isocenter with a constant source to axis distance.

I.6.1 Computed tomography treatment simulation

The virtual simulation is the treatment simulation of patients based solely on CT information. Dedicated CT scanners for use in radiotherapy treatment simulation and planning are known as CT simulators.

Treatment simulation has an important role in the treatment of the patient. It is used for the :

- Determination of the patient treatment position
- Identification of the target volumes and organs at risk

- Determination and verification of the treatment field geometry
- Generation of the simulation radiographs DRRs for each treatment beam for comparison with treatment port films
- Acquisition of patient data for treatment planning

The advantage of virtual simulation is that anatomical information may be used directly in the determination of treatment field parameters [13].

During the treatment delivery the patient is required to stay still therefore during the simulation and depending on the patient treatment position or the precision required for beam delivery, patients may or may not require an external immobilization device (headrest, plastic mask..) for their treatment. Immobilization devices have two fundamental roles:

- To immobilize the patient during treatment;
- To provide a reliable means of reproducing the patient's position from simulation to treatment, and from one treatment to another.

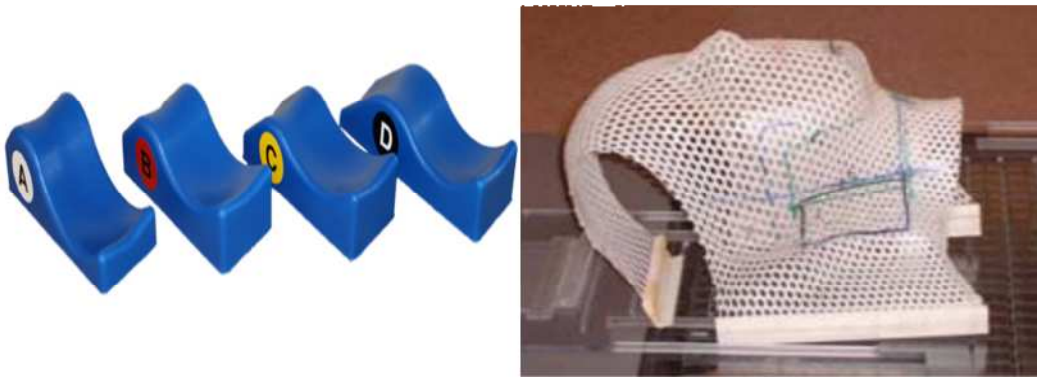

Fig (I.11): Headrests and plastic mask used for patient positioning and immobilization in external beam radiotherapy

I.6.2 Patient Data acquisition in 3D-CRT

Patient data acquisition is an important part of the simulation process, since reliable data are required for treatment planning purposes and allow for a treatment plan to be properly carried out. With the growing popularity of CT in the 1990s, the use of CT scanners in radiotherapy became widespread. Anatomical information on CT scans is presented in the form of transverse slices of the region to be treated, with a suitable slice spacing (typically 0.5–1 cm), which contain anatomical images of very high resolution and contrast, based on the electron density.

The preliminary phase to any external irradiation is done by the oncologist following the clinical examinations. On every CT slice used for treatment planning, the tumour and target

volumes are usually drawn by the radiation oncologist. Organs at risk and other structures should be delineated in their entirety if DVHs are to be calculated.

Other studies are required for image fusion and the results of complementary examinations (CT-scan, MRI, surgery, etc.) and international radiation dosimetry protocols and reports are of great interest.

I.6.3 Volume definition

Volume definition fig (I.12) is necessary for the 3-D treatment planning and for accurate dose reporting. ICRU Reports No. 50 and 62 define and describe several target and critical structure volumes that aid in the treatment planning process and that provide a basis for comparison of treatment outcomes [10].

- **Gross tumour volume:**

The Gross Tumour Volume (GTV) is the gross palpable or visible demonstrable extent and location of malignant growth" (ICRU Report No. 50).

The GTV is usually based on information obtained from a combination of imaging modalities (computed tomography (CT), magnetic resonance imaging (MRI), ultrasound, etc.), diagnostic modalities (pathology and histological reports, etc.) and clinical examination.

- **Clinical target volume:**

The clinical target volume (CTV) is the tissue volume that contains a demonstrable GTV and/or sub-clinical microscopic malignant disease, which has to be eliminated. This volume thus has to be treated adequately in order to achieve the aim of therapy, cure or palliation" (ICRU Report No. 50).

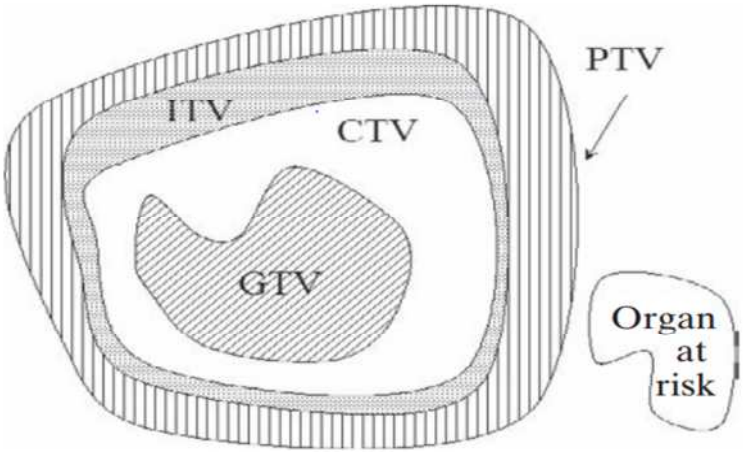

Fig (I.12): Graphical representation of the volumes of interest, as defined in ICRU Reports No. 50 and 62.

The CTV is usually stated as a fixed or variable margin around the GTV (e.g. CTV = GTV + 1 cm margin), but in some cases it is the same as the GTV (e.g. prostate boost to the gland only).

- **Internal target volume:**

The ITV consists of the CTV plus an internal margin. The internal margin is designed to take into account the variations in the size and position of the CTV relative to the patient's reference frame (usually defined by the bony anatomy); that is, variations due to organ motions such as breathing and bladder or rectal contents (ICRU Report No. 62).

- **Planning target volume:**

The planning target volume (PTV) is a geometrical concept, and it is defined to select appropriate beam arrangements, taking into consideration the net effect of all possible geometrical variations, in order to ensure that the prescribed dose is actually absorbed in the CTV" (ICRU Report No. 50).

I.6.4 Organ at risk

The organ at risk is an organ whose sensitivity to radiation is such that the dose received from a treatment plan may be significant compared with its tolerance, possibly requiring a change in the beam arrangement or a change in the dose.

I.6.5 Dose specification

Detailed information regarding total dose, fractional dose and total elapsed treatment days are needed for proper comparison of outcome results. Several dosimetric end points have been defined in ICRU Reports No. 23 and 50 for this purpose:

- Minimum target dose from a distribution or a dose–volume histogram (DVH).
- Maximum target dose from a distribution or a DVH.
- Mean target dose: the mean dose of all calculated target points (difficult to obtain without computerized planning).
- The ICRU reference point dose is located at a point chosen to represent the delivered dose using the following criteria

-The point should be located in a region where the dose can be calculated accurately (i.e. no build up or steep gradients).

- The point should be in the central part of the PTV.

- The isocenter (or beam intersection point) is recommended as the ICRU reference point.

I.6.6 Patient data requirements

Sophisticated treatment planning systems such as used for conformal radiation therapy treatment require specific data for dose calculation:

- The external shape of the patient must be outlined in all area where the beam enter and exit (for contour corrections) and the adjacent areas (to account for scatter radiation)
- The target and internal structures must be outlined in order to determine their shape and volume for dose calculation
- The electron densities for each volume element in the dose calculation matrix must be determined if a correction for heterogeneities is to be applied
- The attenuation characteristics of each volume element are required for image processing

Transverse CT scans contain all the information required for complex treatment planning and form the basis of CT simulation in modern radiotherapy treatment

I.7 Dose calculation Algorithms

The dose calculation algorithm is implemented within the TPS program. It is used at the dosimetry step in radiation therapy planning in order to simulate the patient's treatment and to select the optimised treatment parameters (UM, number of beam and angles, energy and type of IR,) but its main role is to calculate the dose distributions within the patient anatomy.

For a successful outcome of patient radiation treatment it is imperative that the dose distribution in the target volume and surrounding tissues is known precisely and accurately. A typical dose calculation algorithm is required to be both fast and precise at the same time but in reality a compromise between precision and speed of calculation is needed.

- The precision is required to precisely calculate the dose delivered to the tumour target and the organs at risk in order to better control the toxicity effect (NTCP) and the therapeutic effect TCP. The beam's parameters, patient's set-up or even the choice of the algorithm can heavily influence the precision of dose.

- The Speed of the algorithm for dose calculation must be sufficiently fast to ensure a reasonable amount of treatment planning within the day. The time needed for dose calculation is correlated to the power of TPS unit, type of calculating algorithm and the dose calculation matrix (dimension+ resolution).

I.7.1 Types of dose calculation algorithms

The dose calculation algorithms are classified into two main categories:

- ***Correction-based algorithms***: use depth dose data measured in water phantoms (RP, RTM…) with a flat surface and normal incidence to correct with different clinical situation (irregular patient contours, oblique beam incidence, and different tissue densities).
- ***Model-based algorithms***: obviate the correction problem by modelling the dose distributions from first principles and accounting for all geometrical and physical characteristics of the particular patient and treatment.

I.7.2 Commercially available algorithms for clinic use

I.7.2.1 Pencil Beam Convolution algorithm (PBC) with heterogeneity correction

This Pencil beam convolution algorithm (PBC) is a tissue heterogeneity correction based algorithm. With this algorithm the initial dose is computed in a homogenous phantom and corrected by scaling method that uses attenuation modification to consider heterogeneities. The Pencil beam convolution algorithm (PBC) is based on a pencil beam kernel convolution and computes the dose to be delivered to the patient as the superposition of the total energy released per mass unit within an energy deposition kernel. Thus, to model the heterogeneity, the kernels vary with electron density based on the electron density scaling theorem. Heterogeneity corrections are always based on relative electron densities obtained from a CT-Scan.

In this algorithm, heterogeneity corrections are based on relative electron densities obtained from a CT-Scan data. Calculations with density correction were performed using three density correction methods: Batho Power Law (PBC-BPL), Modified Batho (PBC-MB) and Equivalent Tissue Air Ratio (PBC-ETAR). The correction process is based on the addition of a Correction Facto (CF) described for each method in chapter III.

I.7.2.2 Anisotropic Analytic Algorithm (AAA) with heterogeneity correction

Used in the framework of this project, this algorithm is an improvement of the PBC algorithm with modified Batho corrections. This algorithm is introduced in the Varian Eclipse treatment planning system. This algorithm is based on the same PBC model but instead of the pencil beams being derived from measurements, the pencil beams are derived from Monte Carlo simulations. As an improvement of PBC, the anisotropic analytic algorithm (AAA) is able to calculate a lateral scatter component and taking into consideration adjacent tissues densities. The heterogeneity corrections are applied as scaling factors. Dose is then calculated as a superposition of two photon sources (primary and secondary) and an electron contamination source. The photon component is composed of pre-calculated Monte-Carlo scatter kernels, which are then scaled for the patient.

Heterogeneities in the patient are computed by scaling the beamlet primary radiation attenuation by an equivalent depth parameter. The primary Monte Carlo based pencil beams are calculated on a homogenous water phantom and then corrections are applied to consider heterogeneities.

I.7.2.3 Collapsed Cone Convolution (CCC) with heterogeneity correction

Collapsed Cone Convolution (CCC) is an algorithm in clinical use. For dose deposition in a patient the photon beam must first communicate its energy to charged particles which can then deposit dose in a patient. Difference between the total energy released in matter (TERMA) and the kinetic energy released to charged particles (KERMA) is then so evident. The necessary TERMA values are determined for every point within the patient on the basis of the electron density obtained from the CT-scan data. This TERMA data is then convolved with the Monte Carlo point dose kernels and the calculation is performed for the entire patient volume. Dose is calculated in a spherical coordinate system from the point of interaction. These cones are then collapsed into the Cartesian coordinate system of the CT-data to produce a dose distribution in the patient that inherently includes heterogeneity corrections.

I.7.2.4 Acuros XB

This algorithm tries to simulate all the physical processes that beam particles involve – instead of generating beam particles one by one in the simulation process, Acuros XB uses a group of Boltzmann transport equations (BTE) to describe all the physical processes involved,

and these equations are solved using numerical methods. The Acuros XB algorithm is actually implemented in the Varian Eclipse treatment planning system.

I.7.2.5 Monte-Carlo algorithm

Monte-Carlo algorithm is an algorithm started from the first principles of physics. This algorithm simulates the actual physical processes related to dose delivery in external radiotherapy. This process includes two main steps: 1, the radiation beams transport through all the accelerator gantry head components and 2, the collimated beam transport through the patient's body that ensure dose distribution. Some TPS system start be equipped with full Monte-Carlo algorithm.

I.7.3 Algorithms comparison in terms of heterogeneity correction

As it is was accomplished in the framework of this thesis project, the appropriate approach to test and evaluate the accuracy of dose calculation algorithm is to perform measurements and then compare the measured results with the calculated dose in both homogeneous and heterogeneous media . Many works have been done to evaluate the above-mentioned dose calculation algorithms. These algorithms are classified regarding their accuracy from the most accurate to the less accurate as follows: 1. Monte-Carlo algorithm, 2. Acuros XB, 3. CCC, 4 AAA, 5. PBC > [15-20].

Chapter II

In-vivo Dosimetry and TL Dosimetry in External Beam Radiotherapy

II.1 In vivo dosimetry

In vivo dosimetry involves the measurement of radiation doses to patients during their radiation treatment in order to ensure that the treatments are carried out as they were intended. The primary goal of in vivo dosimetry, is quality assurance (QA) of the radiotherapy process.

In vivo dosimetry is used for the overall verification of the chain of treatment preparation and delivery. As such, it measures the radiation dose to the patient, which can be affected by many variables in the overall radiotherapy process. The global results of measurements of patient doses provide the information necessary for assessment of the accuracy and precision in dose planning and delivery for a specific treatment site, or by a given radiotherapy machine.

In vivo dosimetry is an efficient tool for the dosimetric control of the treatment planning system TPS used in external beam radiation therapy to generate beam shapes and dose distributions with the intent to maximize tumour control and minimize normal tissue complications in order to ensure that the therapeutic objectives will be reached

Computerized treatment planning is a rapidly evolving modality, relying heavily on both hardware and software. As such it is necessary for related professionals to develop a workable quality assurance (QA) program that reflects the use of the TP system in the clinic, and is sufficiently broad in scope to ensure proper treatment delivery

One of the most important quality assurances modalities of the In-vivo dosimetry used for TPS dosimetric controls is by the use of the thermoluminescence detectors since they have the advantage of being highly sensitive under very small volume and not to have to be connected to an electrometer with an unwieldy cable [21].

II.2 Luminescence and Thermoluminescence

Some materials, upon absorption of radiation, retain part of the absorbed energy in metastable states. When this energy is subsequently released in the form of ultraviolet, visible or infrared light, the phenomenon is called luminescence. Two types of luminescence, fluorescence and phosphorescence, are known, which depend on the time delay between stimulation and the emission of light.

- Fluorescence occurs with a time delay of between 10^{-10} and 10^{-8} s. The absorbed radiation in the process of fluorescence is spontaneously emitted.
- Phosphorescence occurs with a time delay exceeding 10–8s. The process of phosphorescence can be accelerated with a suitable excitation in the form ofheat or light

If the exciting agent is heat, the phenomenon is known as thermoluminescence and the material is called a thermoluminescent material, or a TLD when used for purposes of dosimetry. On the other hand if the exciting agent is light, the phenomenon is referred to as optically stimulated luminescence (OSL).

II.2.1 Thermoluminescence

Thermoluminescence is thermally activated phosphorescence.Thus, thermoluminescence (TL) is the thermally stimulated emission of light following the previous absorption of energy from radiation. This thermostimulated emission was discovered in the 17th century by Sir Robert Boyle by heating a diamond in the dark. The first theoretical foundations were developed by Urbach (1930), then Randall and Wilkins (1945) who gave a simple scheme, still used in most of the proposed models.Thermoluminescence has various application areas such as, radiation dosimetry, archaeological pottery dating and geology [13].

II.2.2 Theory of thermoluminescence

In a perfect crystal, electrons occupy a number of discrete energy levels distributed in permissible bands separated by forbidden bandsFig.II.1. In a perfect crystal, electrons cannot occupy any energy level located in the forbidden band (FB). At absolute zero, the energy of the electrons is minimal: the conduction band (CB) is empty, and the valence band (VB) is filled. The lower limit of the conduction band is located above the upper limit of the valence band. The energy difference between these bands is called the band gap or energy gap.

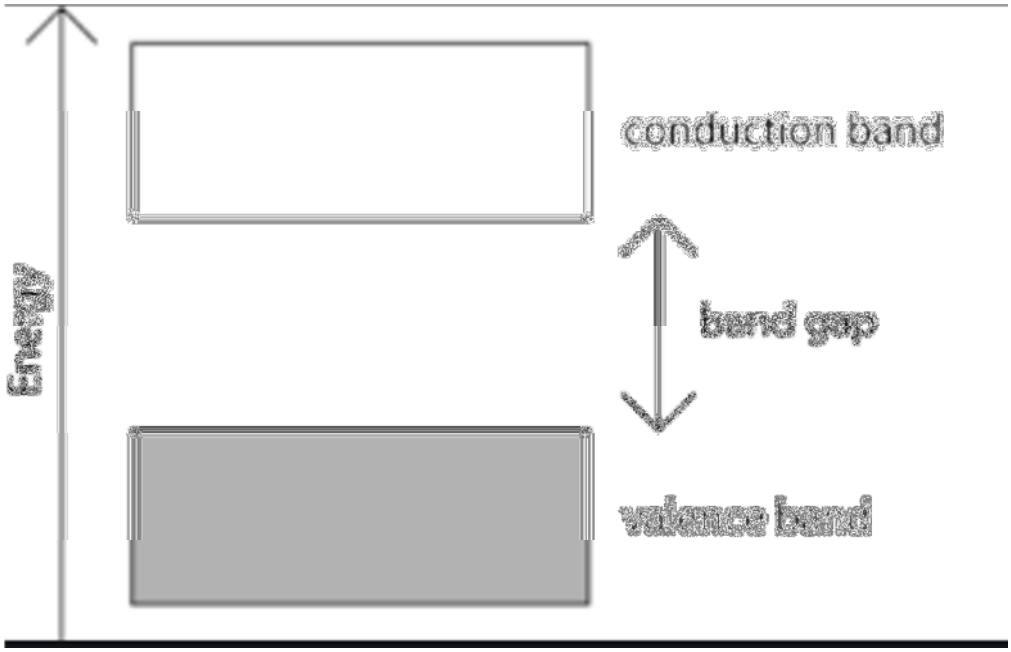

Fig.II.1: conduction bands model

The thermoluminescence phenomenon cannot occur in a perfect crystal because of the wide energy gap. In reality the structure is never perfect due to the presence of a number of lattice defects. Defects (called also traps) introduce additional energy levels to the band gap. The type and the concentration of defects in the crystal can be controlled by the doping with foreign ions. Due to the crystal lattice defects in the energy gap range arise local levels called electron traps if they are close to the conduction band and piercing traps (or simply holes) if they are close to the valence band.

Electrons raised by radiation from valence band into conduction band are captured by the electron traps. Piercing traps, being recombination centers, during heating capture electrons released from electron traps, which during this process give rise to a delayed luminescence light emission.

The thermoluminescence phenomenon is thus a two stage process, where in the exposure and read can be spaced from each other in time. The time distant among the exposure and the readout may be equal to hundreds of thousands or even millions of years.

The first stage is an excitation of the thermoluminescent material by radiation or by light. In that step an ionization of the material occurs, what means that electrons from the valence band or from bands placed deeper are transferred to the conduction band. Some of these electrons from the conduction band can go to electron traps, and the holes left by the electrons migrate to the valence band, passing, partly, into piercing

traps. Depending on the role they play different trap levels are defined as active traps, deep traps and so called recombination centers. At the end of the first stage of TL phenomenon we have a certain number of filled electron traps and piercing traps which is in some range proportional to the absorbed energy.

In the second stage of the TL process due to heating the electrons from traps are transferred to the conduction band, from which they recombine to the recombination centers containing trapped carriers of opposite sign (trap /centers piercing). In the process of recombination the electrons release energy in the form of light, so that the substance returns to its ground state (equilibrium).The energy needed to release trapped carriers is at least equal to the difference between the level of the trap and conduction band (if the "active carriers" are electrons) [22].

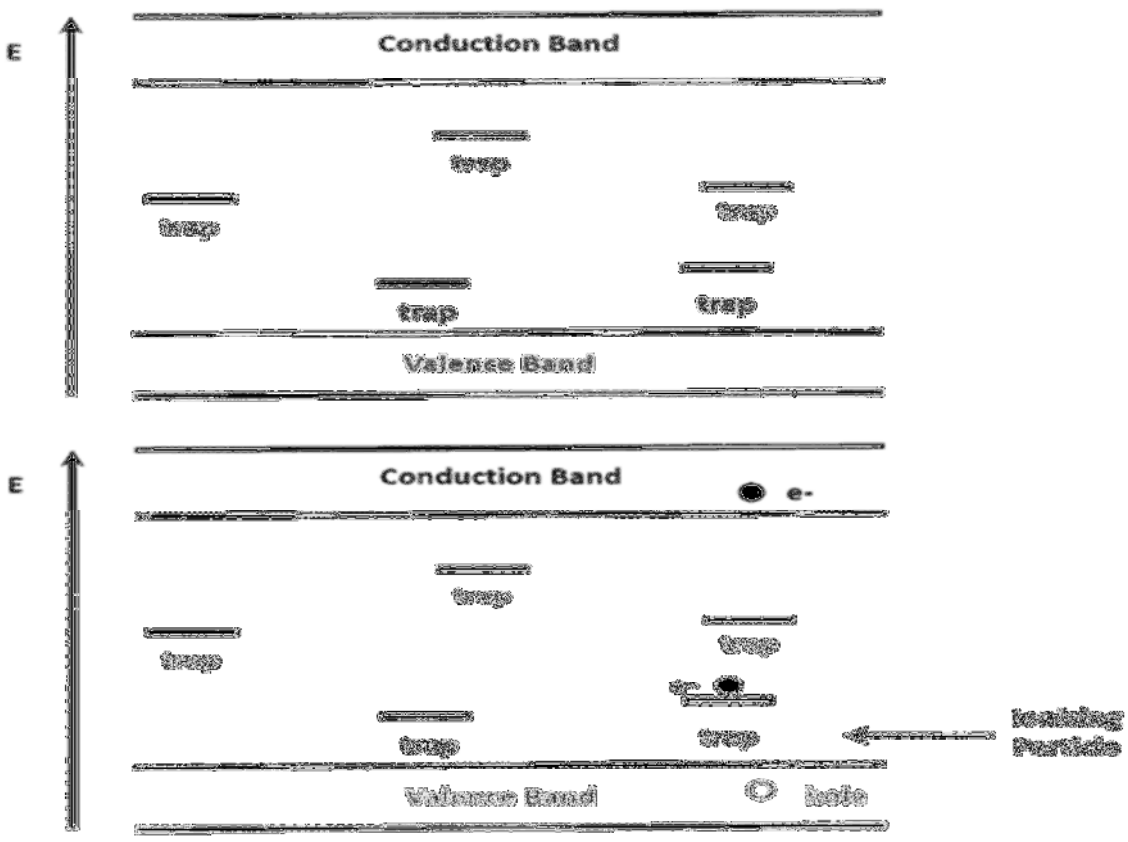

Fig.II.2: (a) TLD crystal structure, (b) electron/hole traps with incoming radiation

The processes of heating and light collection are performed in a readout system called the reader. The signal as a function of temperature is called a glow curve Fig.II.3. It consists of different TL peaks, each peak corresponding to a different energy state in

the crystal. They are either unstable, decaying more or less quickly with time according to the TL material considered, or stable. A TL dosimeter always contains both unstable and stable peaks, the latter (called dosimetric peaks) being the one used in dosimetry. The total thermoluminescence signal emitted (i.e. the area under the appropriate portion of the glow curve) can be correlated to dose through proper calibration.

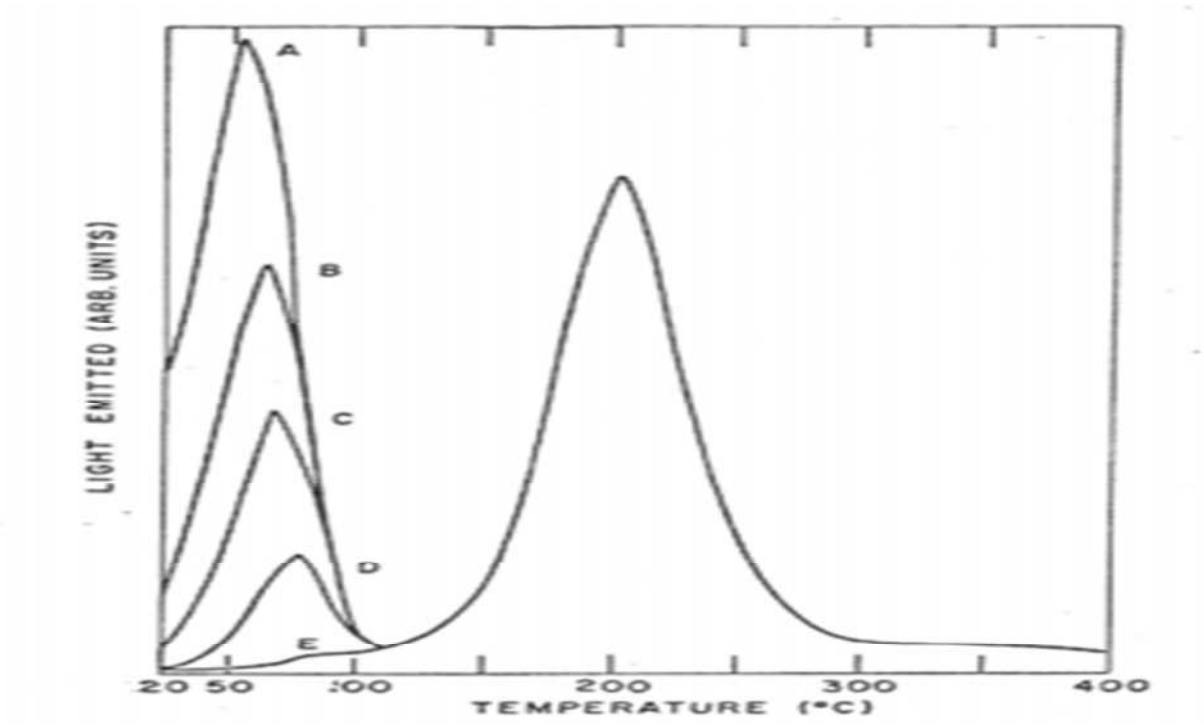

Fig.II.3: The signal as a function of temperature is called a glow curve

After readout, the TL material is either entirely in its original state, and in this case it is just ready for re-use, or it requires a special heating treatment called annealing in order to restore it to its original state.

II.2.3 Basic characteristics of TL dosimeter

1. Signal stability after irradiation

An important consideration in the choice of a TL dosimeter is the stability of the signal. It is necessary to assess whether the charges trapped during the irradiation have not been lost before the readout by unwanted exposure to heat (thermal fading), light (optical fading) or any other factor (anomalous fading). This is expressed by a decrease of the TLD response depending on the delay separating irradiation and readout. Thermal fading should be evaluated on each individual reader with the TL material which is intended to be used.

- Thermal fading can be reduced by an appropriate preheating of the TLD which also allows the elimination of low temperature peaks.
- Optical fading can be avoided by manipulating the dosimeters in a room illuminated with incandescent light and wrapping them in opaque containers or envelopes, when used for in vivo dosimetry in treatment rooms illuminated with fluorescent light.

2. Intrinsic precision

Intrinsic precision is the reproducibility of a given TL material associated with a given readout system. It is very dependent on the quality of the TL material used, reader characteristics, the way in which the preheating and heating cycle have been defined, the purity of the nitrogen gas circulating in the readout chamber.

It can be evaluated by selecting a number of TL dosimeters out of the same batch and by irradiating them to the same dose. After readout, and annealing procedure when necessary the operation is repeated several times.

When readout parameters have been optimised, TL materials which show a standard deviation higher than + 2 % are either of poor quality or are not correctly handled and read out. They should not be used for in vivo measurements or the handling procedure should be improved.

3. Sensitivity: identification of dosimeters

Some variations in sensitivity within a batch of TL dosimeters is unavoidable. Several methods can be used to limit the effect of these variations when the dosimeters are in common use. The best method consists of irradiating all the dosimeters in the same geometrical conditions, to read them out and to attribute to each of them a sensitivity factor Si equal to:

$$S_i = \frac{R_i}{\bar{R}}\,, \qquad \text{(II.1)}$$

Where Ri is the TL readout from dosimeter number i and $\bar{R}$ the mean of all values of R_i.This sensitivity factor expresses the response variation of each individual dosimeter around the mean. Although this mean may vary from irradiation to irradiation, Si should remain constant because all dosimeters are subject to the same variations. Sensitivity factors should be checked periodically to take into account a possible loss of material occurring when TL dosimeters are not handled carefully.

4. Influence of the dose

The TL emission per unit of absorbed dose is illustrated by the typical curve shown in Fig (II.4). In practice it is recommended to use TL dosimeters in the region where their response is proportional to the dose received (linear region). When it is not the case, a correction

should be applied to the signal from a curve established with the TL material as well as the reader used. This curve should be checked periodically and the TL dosimeters should not be used in the sublinear region approaching saturation.

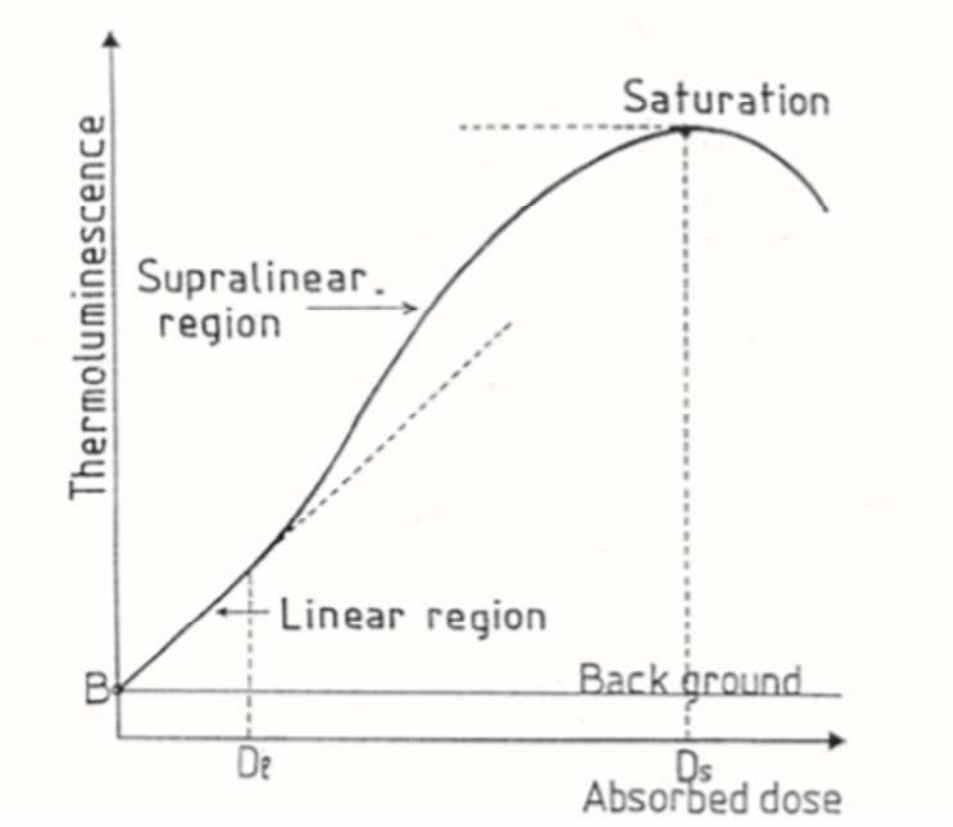

Fig.II.4: Variation of thermoluminescence as a function of absorbed dose

5. Influence of the dose-rate

TL dosimeters are to a large extent dose-rate independent. This property implies in practice that the dose-rate variations produced by beam modifiers, SSD variations, patient thickness, etc. do not have to be taken into account with the TL method. Even the extreme high dose-rates produced in scanned electron beams of linacs do not cause any special difficulty. No correction for dose-rate is necessary in the range of clinical dose-rates applied.

6. Influence of the temperature

As the temperatures is required to get the light signal out of the TL crystal is high compared to room or patient temperature, the response of TL dosimeters is independent of temperature variations in the range concerned by in vivo dosimetry. However care should be taken not to store the dosimeters close to a heat source. No correction for temperature is necessary for in vivo dosimetry.

7. Directional effect

The intrinsic response of TL dosimeters is not influenced by the direction of the beam. No correction for directional effect is necessary except if the dosimeter container and associated build-up cap have an asymmetric shape; even for the tangential irradiation of the breast or the thoracic wall no directional dependence of detector response is observed.

II.2.4 Types of TL detectors and uses

TLDs are available in various forms (e.g. powder, chips, rods and ribbons).Most commonly used TL detectors are obtained by doping phosphors such as lithium fluoride (LiF), lithium borate (Li2B407), calcium sulphate (CaSO4) and calcium fluoride (CaF2) with impurities called activators: e.g.Li2B407:Cu is lithium borate doped with copper, etc. The most commonly used TL material is the lithium fluoride LiF. There are several detectors on its basis, especially such as: LiF:Mg,Ti (called MTS) and LiF: Mg,Cu,P (called MCP).

The thermoluminescent materials used in the industry have three major areas; radiation dosimetry, age determining and geology. Radiation dosimetry has three subgroups; personnel dosimetry, medical dosimetry and environmental dosimetry. The ones being related to Medical field are personal and medical dosimetry

1. TLD use for personnel dosimetry

Personnel dosimetry is used in areas where the personnel are exposed to radiation in nuclear reactors, radiology and radiotherapy facilities in hospitals or such. Besides, from the constant radiation exposure, there are accidental or incidental radiation exposures, which are also measured by personnel dosimetry. The purpose of using personnel dosimetry is to keep track of the radiation exposure level of the individual to avoid averts radiation based effects.

Personnel dosimetry has three sub categories; extremity dosimetry, whole-body dosimetry and tissue dosimetry.

Extremity dosimetry focuses on body parts that are exposed to radiation such as hands, arms or feet while the whole-body focuses on the tissue below the surface of the body or the critical organs. It measures the dose absorbed in these parts of the body by dealing with gamma and X- rays (greater than 15 keV) and neutrons which are penetrating rays.

Tissue dosimetry also called skin dose, measures the dose absorbed by skin. It focuses on non-penetrating radiation such as beta particles or <15 keV X-rays

2. TLD use in medical dosimetry

Medical dosimetry intends to measure the effects of a TLD that is placed into the appropriate places within human body undergoing diagnosis or treatment by any ionizing radiation

device. Before exposing the patient to any IR or during first sessions of irradiation (In-Vivo dosimetry for treatment quality assurance), measurements can be made upon these TLD and from the data obtained, possible additional treatments or dose control can be implemented.

In order for these measurements to be done, a thermoluminescence dosimetry (TLD) material that is equivalent to the human tissue is needed. The TLD material should absorb the same dose or amount of radiation as the human tissue would do in the same area within the same radiation levels. Among available TL materials those which can be considered equivalent to soft tissues or to bones in the energy rang encountered in radiation therapy are listed in table (II.1)

The TLD should also be highly sensitive for measurements done in laboratory conditions that require the possible smallest size of TLD material.

Table (II.1): Different TL materials equivalent to soft tissues, lungs or bones

Soft tissue or lung	Bone
LiF (Mg, Ti) LiF (Mg, Ti, Na) $Li_2B_4O_7$: Mn $Li_2B_4O_7$: Cu	$CaSO_4$: Mn $CaSO_4$: Dy CaF_2 : Mn CaF_2 : Dy

CHAPTER III

Heterogeneity Correction in External Radiotherapy

III.1 Dose calculation in presence of Heterogeneities

Successful treatment in radiotherapy is closely related to the evaluation of the treatment planning based on the principle of delivering the maximum dose to the tumor while sparing the surrounding normal tissue and organs at risk (OAR) such as the heart, the spinal cord, healthy lung tissue and any other organ that is not affected by the tumor being treated. Depending on the location of the tumor and the surrounding OARs, several plans may be considered. These plans must be evaluated in order to select the best one that is conforming to the specified dose delivery criteria and the OARs protection [23]. The medical physicist with the assistant of the clinician has, thus, to evaluate the treatment plans and to perform the necessary corrections to address any wrong situation. Any correction must be performed on the basis of the used treatment planning algorithm and the reconstructed CT scan data.

In radiotherapy there are many available treatment planning systems, all are based on the same radiation interactions but differ in dose calculation approaches. These algorithms used measurement data (depth dose profile, isodose curves ...) obtained by the consideration of homogenous medium (water phantom). The human body cannot be considered as homogenous in all treatment cases because the presence of bones and air cavities. These heterogeneities can affect considerably the treatment plan and must be taken into consideration for the treatment planning. This is why practically all the treatment planning system (TPS) includes in addition the main dose calculation algorithm some addition algorithms particularly used to address this issue.

III.2 The Heterogeneities in human body

Generally, in the human body, tissues whose atomic number and density are different of those of water are called heterogeneities. The human body contains numerous heterogeneities (lung, oral and nasal cavities, tooth, bone, possibly prosthesis...). These heterogeneities can be easily identified and therefore separated from the homogenous tissues by CT-scan which allows obtaining a map of the attenuation coefficients, or rather in Hounsfield unit (HU). Thus, the Hounsfield unit is a manner to compare the attenuation of the X-rays through different tissues, and is given by:

$$HU = 1000\,\frac{\mu_{tissu}-\mu_{water}}{\mu_{water}} \qquad \text{(III.1)}$$

In the Megavolt energy range used in radiotherapy with a predominant Compton interaction effect, the important element to take into account for the calculation of the dose in the patient is the electronic density of the medium defined by the number of electrons per unit volume. The obtained HU mapping by the scanner is transformed by the TPS to electronic density mapping using a correspondence curve (Fig.III.1) [24].

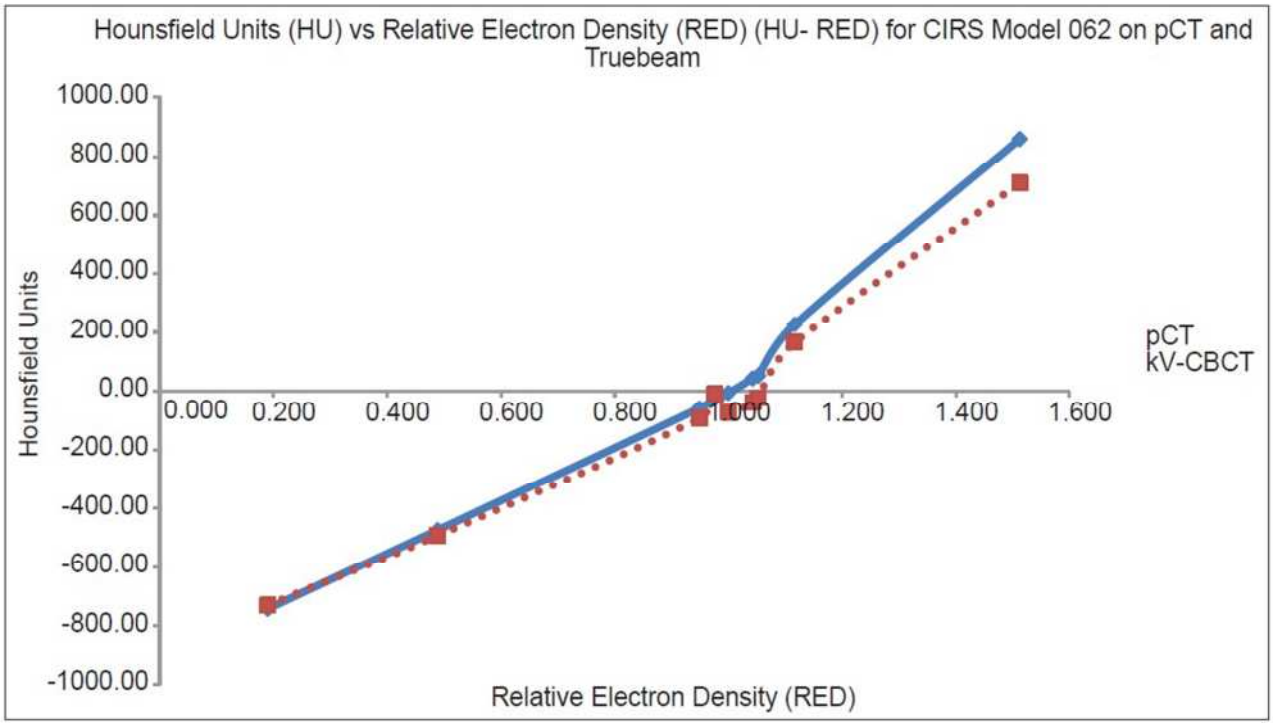

Fig. III.1: Typical HU-Electron density curve of CIRC model 62 phantom [24].

F. Tatsugami et al. have measured the electron density of numerous biological tissues using dedicated phantom and compared the obtained values to the true values (Table (III.1)) [25].

Table III.1: The true and measured electron densities and the errors between the true and measured values [25].

Inset number	Real tissue Substitute	Physical Density [g/cm³]	True electron density (Relative to water)	Mean measured electron density (Relative to water)	Error [%]
1	LN-300 Lung	0.290	0.282	0.296	5.08
2	Solid Water	1.019	0.990	0.999	0.95
3	Inner Bone	1.129	1.082	1.078	-0.38
4	Solid Water	1.019	0.990	0.996	0.58
5	Liver	1.094	1.062	1.066	0.39
6	Bone Mineral	1.146	1.099	1.094	-0.49
7	LN-450 Lung	0.450	0.435	0.454	4.36
8	Solid Water	1.019	0.990	0.998	0.80
9	Brain	1.053	1.049	1.045	-0.34
10	Adipose	0.941	0.924	0.935	1.19
11	CB2-50%	1.561	1.471	1.439	-2.18
12	Solid Water	1.019	0.990	0.993	0.34
13	CB2-30%	1.234	1.179	1.158	-1.83
14	True Water	1.000	1.000	1.000	0.00
15	Breast	0.980	0.957	0.962	0.53
16	Cortical Bone	1.821	1.693	1.659	-2.03

III.3. Influence of the heterogeneities on dose Distribution

Heterogeneity in the irradiated medium can modify the type of interactions of the particles of the primary beam with the material (PE effect, Compton and Materialization) which is closely dependent on the atomic number Z of this heterogeneity medium. The nature of the particles (electrons or photons) constituting the scattered radiation, their energy, their number and their type of interaction, will also be modified. The dose distribution will then be impacted particularly inside and after heterogeneity medium. The following effects and impacts generally happen if heterogeneity exists in the irradiated medium:

1. ***Before the heterogeneity (weak impact)***: generally the primary beam is not affected but closely to heterogeneity the backscattered beam is slightly modified.

2. ***Inside the heterogeneity:*** Primary beam considerable affected by the attenuation inside the heterogeneity. The dose distribution is mainly affected by the secondary

electrons fluence variation. In the electron equilibrium zone, the dose correction is given by:

$$\frac{D_{heter}}{D_{water}} = \frac{(\frac{\overline{\mu en}}{\rho})_{heter}}{(\frac{\overline{\mu en}}{\rho})_{water}} \qquad \text{(III.2)}$$

Where: D_{heter} is the dose in the heterogeneity medium, D_{Water} is the dose if medium is homogenous water medium, $\frac{\overline{\mu en}}{\rho}$ is the mass attenuation coefficient of the energy absorption in the considered medium (heterogeneity and water).

At the heterogeneity interfaces, the electron non-equilibrium zone is modified because the secondary electrons paths are modified.

3. ***After the heterogeneity*:** In this zone, the dose distribution is strongly affected because the attenuation of primary beam attenuation is mainly changed. Close to heterogeneity interfaces, the backscattered beam is less affected by heterogeneity.

Examples on how heterogeneity can seriously affect the percent depth dose profile (PDD) in a specific case of radiotherapy are presented in figures (III.2) and (III.3) [26].

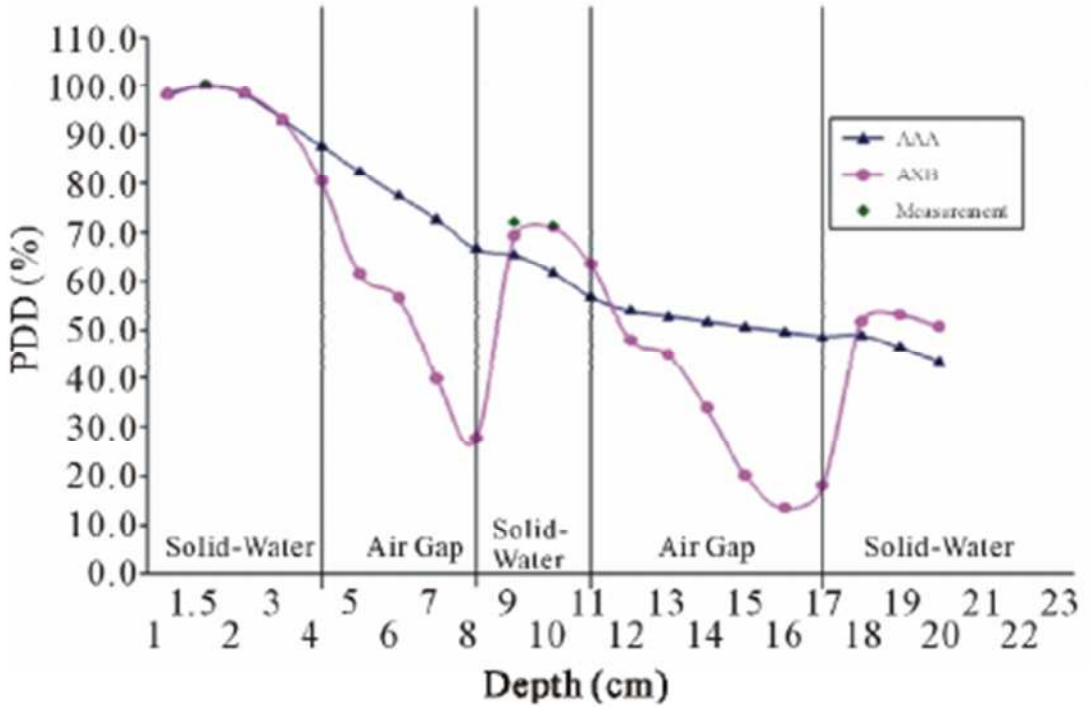

Fig. III.2: The calculated PDD curves by AAA and AXB algorithms and the measured PDD in a heterogeneous rectangular slab phantom [26].

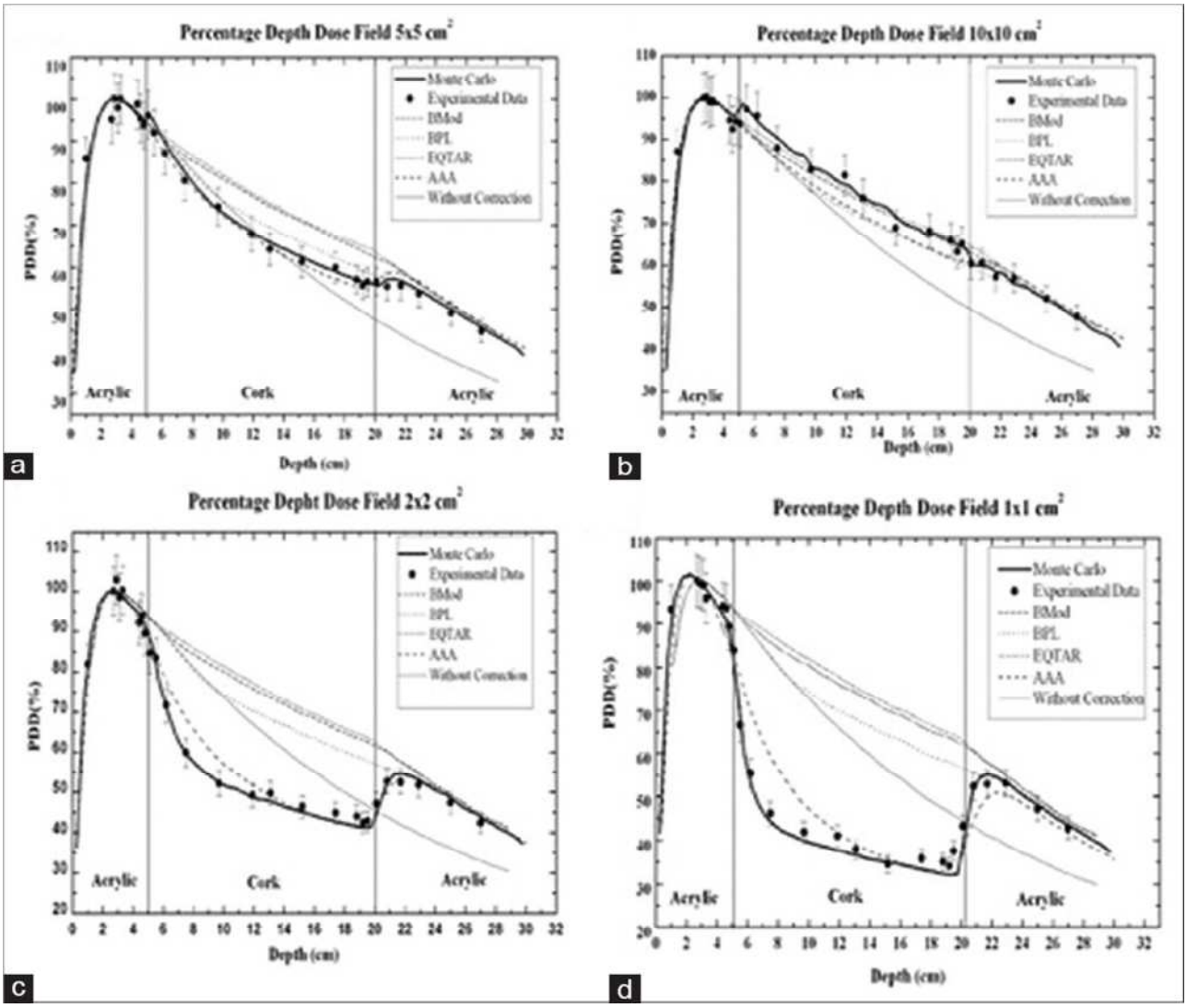

Fig. III.3: PDD curves calculated through the radiotherapy Eclipse planning system algorithms Batho, modified Batho, equivalent TAR, and anisotropic analytical algorithm (AAA); measured with thermoluminescent dosimetry and simulated using EGSnrc Monte Carlo code for a irradiation field of (a) 10 × 10 cm^2, (b) 5 × 5 cm^2, (c) 2 × 2 cm^2, and (d) 1 × 1 cm^2 [27].

III.4. Taking into account heterogeneity in dose calculation

By taking into account the heterogeneities in dose calculation contributes essentially to know precisely the received dose by the target volume (s) and the OARs of the patient and thus to better control the radiotoxicity and the therapeutic effects of the radiation treatment. Indeed, it is very important to take into account the heterogeneities particularly when using a modern radiotherapy treatment technique such as 3-dimensions conformal radiotherapy (RC3D) or intensity modulation radiotherapy (IMRT) because the conformation of the isodoses of high

level of dose to the target volumes is more precise and thus a difference of some millimeters on the calculated dose may be enough to under treat one part of the target volume.

III.5 Heterogeneity correction methods for dose calculation

The heterogeneity dose correction process can be applied in two manners:

1. **The indirect method**: The first calculation is performed by considering a homogeneous medium (water, d = 1g/cm^3), then the obtained distribution of is corrected by applying a corrective factor (*CF*) to deduce the distribution of the dose in the heterogeneous medium. The dose in heterogeneous medium at a point *P* (D_{heter}) is then given by:

$$D_{heter}(P) = CF(P).D_{homo}(P) \qquad \text{(III.3)}$$

Many methods are available to determine *CF* such as:

- ***The Tissue–air ratio (TAR)*:** method where the *CF* is given by:

$$CF = \frac{TAR(\grave{z},r_d)}{TAR(z,r_d)} \qquad \text{(III.4)}$$

Where $z\grave{} = z_1 + \rho_e z_2 + z_3$, $z = z_1 + z_2 + z_3$, z_i is the depth distance before, inside and after the heterogeniety, ρ_e is the electron density of the heterogenity and r_d is the radiologic distance.

This method does not account for the position relative to the inhomogeneity (z_2). It also assumes that the homogeneity is infinite in lateral extent.

- ***The Batho power law method***: method initially developed by Batho [28] and developped by Sontag and Cunningham [29].The dose at any point *P* below the heterogeneity is corrected by:

$$CF = \frac{TAR(z_3,r_d)^{\rho_3-\rho_2}}{TAR(z,r_d)^{1-\rho_2}} \qquad \text{(III.5)}$$

Where $z = z_1 + z_2 + z_3$, ρ_1 is the relative electron density of the medium in which the point *P* is considered, ρ_2 is relative electron density of the overlying material (heterogeneity).

At the opposit of the last method, this method take into account the position relative to the heterogeneity. It also still assumes that the homogeneity is infinite in lateral extent.

- ***Equivalent tissue–air ratio method***: This method is is similar to the TAR method described above, with the exception that the field size parameter is modified as a function of the relative density to correct for the geometrical position of the heterogeneity with respect to the calculation point *P*. The dose at any point P is corrected by:

$$CF = \frac{TAR(\dot{z},\grave{r_d})}{TAR(z,r_d)} \qquad \text{(III.6)}$$

- ***Isodose shift method:*** This method is identical to the isodose shift method used for contour irregularities. Isodose shift factors for several types of tissue have been determined for isodose points beyond the heterogeneity. The factors are energy dependent but do not vary significantly with field size.The factors for the most common tissue are presented in table (III.2). The total isodose shift is the thickness of inhomogeneity multiplied by the factor for a given tissue. Isodose curves are shifted away from the surface when the factor is negative.

Table (III.2): The correction factors for the most common tissue and energy [34].

Energy	%/cm Correction	
	Lung	Bone
Cobalt-60	+4.0%	–2.5%
4–6 MV	+3.0%	–2.0%
10 MV	+2.5%	–1.5%
18–25 MV	+1.5%	–1.0%

2. **The direct methods:** the calculation is done directly in a heterogeneous medium. Only full Monte Carlo algorithms explicitly account for heterogeneities, the others methods and models of radiation transport use approximate correction methods that are generally based on Fano and O'Connors theorems.

- ***Fano theorem:*** As it is well established, the dosimetric data used in treatment planning are mainly derived from water. The existence of two important theorems of radiation transport for photons and for charged particles by O'Connor and Fano enables density scaling of data for water to "water-like media" with arbitrary densities**.** This theorem assumes that for in an infinite medium of constant atomic composition exposed to uniform radiation (photon) fluence, the secondary radiation fluence (electrons) is also uniform and is independent from the density and its variations from one point to another. This constant fluence of secondary electrons equals the fluence generated under conditions of charged particle equilibrium (CPE) for a given fluence of photons. Consequently, the absorbed dose across any area of density variations would be constant. This is intuitively plausible since density not only modulates the number of electrons launched per unit volume, but also rescales their linear range. The main assumption in Fano's theorem is that the interaction cross sections per unit mass are independent of the density of a medium of identical atomic composition [30].

- ***O'Connor theorem:*** In this theorem it is supposed that if two media of different densities but of identical atomic composition are irradiated by the same beam, the dose at the corresponding points in the two media is the same if all the geometric distances (including the field size and the DSP) are dimensioned with a manner inversely proportional to the density as shown in figure (III.4). , Most algorithms use it directly or indirectly to transport photons [31].

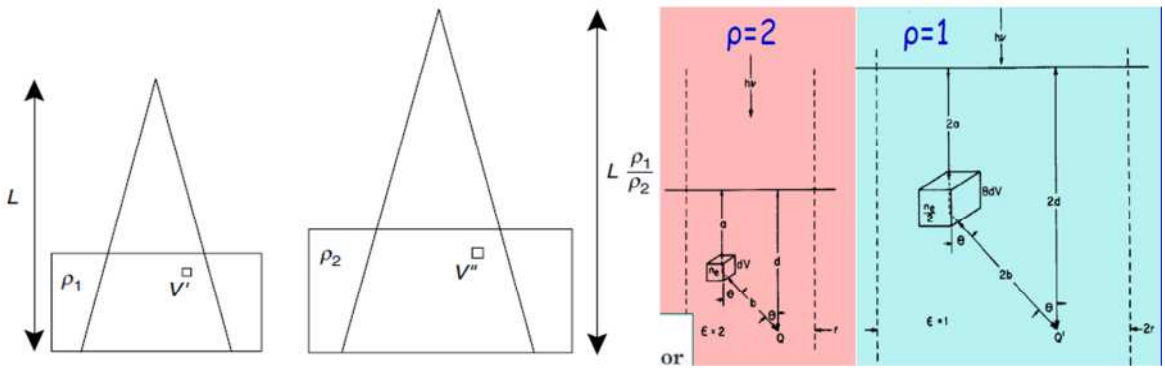

Fig III.4: O'Connor theorem illustration

- ***Theorem of reciprocity*:** This theorem specifies that reversing the positions of a point detector and an isotropic point source within an infinite homogeneous medium does not change the amount of radiation detected. It is strictly valid only for mono-energetic beams. It serves as a basis and justification for necessary beam's data calculation used in kernels superposition/convolution methods such as "kernel pencil beam" and particularly when the dose is to be measured in small region instead the patient body by kernel inversion (Fig III.5) [32, 33].

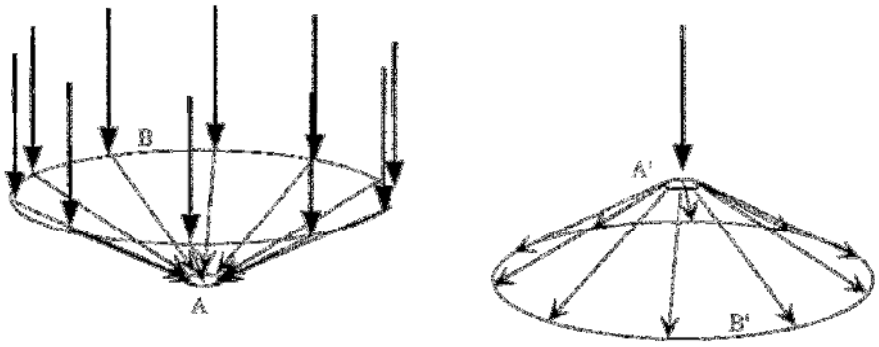

Fig III.5: The estimate of dose originating from a large scattering element *B* to a small element A, as shown to the left, can be made with better scoring statistics by use of a reciprocal geometry as to the right in which *A'* is used as the scattering element and *B'* as the tally region. The set-up requires a homogeneous medium and rotational symmetric scattering around the primary particle direction for the reciprocity to apply [32, 33].

III.6 Correction Methods classification regarding the AAPM report 85

The heterogeneity correction methods and algorithms are classified by the American Association of Physicists in Medicine (AAPM) into four main catgories. Each categorie includes many 1D and 3d correction methods [34].

1. **Category 1: Local Energy Deposition**

In this category the electron tranport is not included.

- **1D Density Sampling:** The models in this method assume that the patient consists of a semi-infinite slab geometry per calculation point, and all energy from the photon

interactions is deposited at the site of interaction**.** Only primary ray-tracing is used to calculate the dose to a point.

- **Method 1.1-Linear attenuation**: Very simple method of heterogeneity correction by adjusting the dose at a given point by on the basis of the overlying thickness of the heterogeneity and by some percent per cm distance correction factor (Eq. III.3).

- **Method 1.2- Effective attenuation coefficient**: The effective attenuation coefficient and the point correction is given by:

$$CF = e^{\mu'(d-d')} \qquad \text{(III.7)}$$

where: μ' is the effective attenuation coefficient of water for a particular beam quality, d is the physical depth from the surface to the point of calculation, and d' is the radiological depth given by:

$$d' = \sum_i \Delta d_i . \rho_i \qquad \text{(III.8)}$$

Where: Δd_i are the thicknesses of tissues with different relative electron densities ρ_i lying above the point of calculation.

- **Method 1.3-Ratio of tissue-air ratios (RTAR)**: already described above**.**

- **Method 1.4-Power law (Batho)**: already described above.

2. Category 2: Local Energy Deposition

This category too doesn't include the electron tranport.

- **3D Density Sampling**:

With these methods the assumption of slab-like geometry is overcome because the heterogeneity intercepts only a portion of the radiation beam. 3D density information of the scattered photon dose is then considered. Here, the electron equilibrium is assumed or the supposition that the electrons are absorbed at the point where they are created is considered.

✓ **Method 2.1-Equivalent tissue-air ratio (ETAR)**: method implemented in commercial treatment planning systems during the 1980s and is still in use on a number of modern systems [35]. First practical dose calculation method using the full CT data set for computerized treatment planning. The ETAR correction factor for homogeneous, non-unit-density water-like medium is given by:

$$CF = \frac{TAR(\rho d,\rho r)}{TAR(d,r)} \qquad \text{(III.9)}$$

Where: $TAR(\rho d, \rho r)$ is the tissue air ratio in a field of radius r at depth d in a uniform medium of density ρ relative to water and $TAR(d,r)$ the tissue air ratio in a field of radius r at depth d in a water (ρ=1).

The application of ETAR method to *heterogeneous* geometries is given by:

$$CF = \frac{TAR(d\prime,r\prime)}{TAR(d,r)} \qquad \text{(III.10)}$$

Where d' and r' are the scaled or effective values of d and r respectively for the energy of the radiation being used. d' is derived by averaging CT values along primary photon ray paths.

✓ **Method 2.2-Differential scatter-air ratio (dSAR):** Method developed by Beaudoin 1968 which demonstrates that it was possible to use scatter-air ratios to calculate the dose to a point in a heterogeneous medium [36]. Thus scatter contribution that arises from voxels within the irradiation volume is determined by a scatter-air ratio table differentiated numerically in the depth and lateral r directions. The scatter from such an elemental volume ΔV is dependent on five: the attenuation of the primary to the scattering volume ΔV; the number of photons per electron of ΔV emitted; the attenuation and geometrical dispersion of the scattered photons; the absorbed dose per unit fluence; and the electron density of the volume ΔV. Due to the available CT technology and weak calculation tools during this period, this method was never implemented clinically.

✓ **Method 2.3-Delta volume (DVOL):** Developed by Wong and Henkelman in 1983 on the basis the dSAR [37, 38]. This method considers a primary and an analytical first scatter calculation and, then, a term containing SARs and a residual scatter component is determined experimentally. Two limiting conditions that should be met by all photon dose calculation algorithms: accurate prediction of dose and the homogeneous, non-unit density medium. This

method is not used clinically because the improved accuracy needs very long calculation times (3D volume integration) during this period (80s).

✓ **Method 2.4-Differential tissue-air ratio method (dTAR):** Developed by Kappas and Rosenwald, this method proposes a simplification of the differential scatter-air ratio method (dSAR) that gives more accurate results [39]. The simplification of the dSAR method essentially consists in suppressing the multiplicative factor which accounts for the lateral distance between the primary interaction and the calculation point.

✓ **Method 2.5: 3-D beam subtraction method:** This method was proposed by Kappas and Rosenwald and tries to ameliorate the methods of category 1 by taking into account the following:

✓ The point of calculation is not necessary located on the beam axis,

✓ The primary is not always affected by the presence of the heterogeneity,

✓ The lateral dimensions of the heterogeneity could be smaller than the field dimensions.

This method consists of using a mathematical combination of on-axis conventional (category 1) correction factors [40]. It is very fast and comparable in performance with the Batho method with no additional data requirements.

3. Category 3: Non-Local Energy Deposition

This category of methods includes the electron transport.

➢ **1D Density Sampling**

- **Method 3.1-Convolution techniques:** This method takes its name from convolution mathematical technique that governs the dose calculation algorithm where the energy fluence distribution is convolved with the scatter spread kernel to obtain dose. These kinds of methods are still available on many TPS. That use convolution/superposition dose calculation algorithms.

- **Method 3.2-Fast Fourier Transform (FFT) convolution:** The FFT convolution method was introduced by Boyer et al [41]. The dose for for a polyenergetic beam spectrum is given by:

$$D(\vec{r}) = \sum_n \int_v \emptyset_n(\vec{r}').K_n(\vec{r} - \vec{r}')dV \qquad \text{(III.11)}$$

Where: $K_n(\vec{r} - \vec{r}')$ is the dose spread kernel for the nth energy interval, and $\emptyset_n(\vec{r}')$ is the spectrally weighted primary fluence.

This method can compute the dose very accurately in areas of electronic disequilibrium although they may not represent in most cases internal heterogeneities.

4. Category 4: Non-Local Energy Deposition (Electron Transport)

➢ **3D Density Sampling**

This category of heterogeneity correction methods employs complex models to incorporate 3D density CT information for the transport of both scattered **photons** and electrons. These methods include the dose spread array (DSA) method developed by Mackie et al. [42], the differential pencil beam (DPB) method by Mohan et al. [43], the convolution method using total energy released in the medium (TERMA) concept of Ahnesjo et al. [44], the forward and backward scatter transport model of Iwasaki [45], and the Woo et al. method implemented in Theraplan-Plus (MDS-Nordion) [46].

- **Method 4.1-Superposition-convolution methods:** The superposition and convolution is a widely used principle for dose calculation in radiotherapy. The correction principle is based on the account for tissue heterogeneities that deform both the TERMA distribution and the dose spread kernels. Indeed, tissue that is in the path of the primary ray influence the TERMA at each point in the patient. Thus, the primary beam penetration is calculated by ray-tracing through the voxel densities in the 3D volume along divergent beam ray paths [47]. The convolution/superposition is the integration of the TERMA distribution multiplied by the kernel over the entire patient volume. In general, the effective density calculated along the scattered ray path is used to change secondary particle contributions or to look up the appropriate value in the scatter kernel using density scaling. Many analytical methods were developed and actually used under this category.

- **Method 4.2-Monte Carlo dosimetry in heterogeneous media:** The Monte Carlo method is a connexion between measurements and analytically based numerical calculations. Dose perturbations at a heterogeneity interface are due to a number of complex effects that are related to the difference in the attenuation coefficients, the mass energy absorption coefficients, and the mass collision stopping powers on either side of the heterogeneity interface. For Monte Carlo simulation accurate charged-particle transport is important because charged particles set in motion on one side of the interface can migrate to the other side and deposit energy. Several Monte Carlo codes have been used with success in supporting, testing, or guiding the development of dose calculations for radiotherapy applications especially for complex tissue interfaces problems [48-50]. Actually, some TPS are working with a Monte Carlo calculation option but Monte Carlo may be of more benefit for electron beam planning than for photons.

CHAPTER IV

Comparison of measured and calculated doses in a Rando phantom with a realistic lung radiotherapy treatment plan including heterogeneities

IV.1 Objective

This study aimed to examine the compatibly of the AAA-calculated and TL-measured doses and therefore to evaluate the Eclipse-Varian TPS performance. Thus, it was also a question to check if the treatment plans validated during the calculation phase was valid by TL measurement according to the ICRU recommendations on dose delivery to the PTV reported in reports 50 and 62 [9-10]. In this context, ICRU recommends that the delivered doses to PTV must be within the interval of 95% to 107% of the prescribed dose. Since the prescribed dose is 2Gy per session, calculated or measured doses must be within the dose interval of [1.9Gy-2.14Gy]. Thus, an accuracy of -5% to +7% in the delivered absorbed dose to PTV is required.

In this work, indirect TL dosimetry at different depths was performed using a Rando phantom instead of a real patient. Therefore, a virtual patient was created within the Eclipse treatment planning system (TPS) on the basis of computed tomography (CT) data of the Rando phantom. Real structures and programmed fields of a real patient were copied on the virtual patient by performing all the necessary image-registration and fusion adjustments within the TPS. Based on the dose prescribed for the real patient, a new treatment plan and dose calculation was performed for the virtual patient (Rando phantom) using the AAA algorithm modified by transversal, lateral and at the interface dose heterogeneity corrections [8]. Patient treatment plan was generated with 6MV co-planar three-field beams optimized with tissue heterogeneity correction to deliver a prescribed dose of 40 Gy in 20 fractions.Some updated dose-delivery constraints for the studied case were considered such as the delivery of 95% of the prescribed dose to95% of the planning target volume (PTV), the delivery of less than 17Gy (42.5%) to the heart and the delivery of less than 10Gy (25%) to the spinal cord [51]. Doses were calculated by the TPS with and without heterogeneity correction, to get an idea about the performance of the heterogeneity correction algorithm in different situations (tumour volume, structures or organs, etc.). Finally, doses were measured in 19 well selected positions where TLDs can be placed within the Rando phantom. The TLDs weredistributed on threephantom's layers corresponding to the following CT-slices: 6.3cm, 9 cm and 12.3cm (Z-position).

The comparison between doses calculated and doses measured by means of thermoluminescence (TL) shows compatibility except for a few points, due to the limitations in the heterogeneity correction used for the case studied here. The deviation between

calculated and measured doses is about 6.5% for low (<0.5Gy) doses, and about 1% for higher doses (>0.5Gy).The deviation between AAA-calculated and TL-measured doses were also found to be higher in proximity to heterogeneous tissue interfaces.

IV.2 Material and Methods

IV.2.1 Material

IV.2.1.1The Linear accelerator LINAC

Linacs are used in radiation therapy to produce high energy ionizing radiation (up to 25MeV). The Linac Varian Clinac® iX SN5818 is used in this study (Fig. IV.1). The technical specifications of this accelerator are:

- Energy photons: X6 and X18 MV.
- Electrons Energy: 6, 9, 12, 16 and 20 MeV.
- Dose rate: 100 to 400 MU/min (MU: monitor unit).
- Multi-collimator leaf (120 leafs)

Fig.IV.1: LinacVarianClinac® iX SN5818

IV.2.1.2 The RANDO phantom

The RANDO® Phantom is an invaluable aid in radiotherapy treatment planning. It enables detailed mapping of dose distribution. This detailed dose information is useful for patient treatment evaluation, quality assurance of automated treatment planning systems and research

The RANDO® male model used in this study represents a 175cm tall and 73.5kg male figure (Fig IV.2). The figure is with no arms or legs. The phantom is transected horizontally into 2.5cm thick slices. Each slice has hole grid patterns which can be drilled into the sliced sections to enable the insertion of TLD dosimeters. Two tissue-simulating materials are used to construct the RANDO Phantom: the RANDO soft tissue material and the RANDNO lung material. Both of these are designed to have the same absorption as human tissue at the normal radiotherapy exposure levels. Phantom is constructed with a natural human skeleton which is cast inside soft tissue-simulating material. Lungs are molded to fit the contours of the natural rib cage.

Fig. IV.2: The RANDO® male model

The soft tissue material has an effective atomic number and mass density which simulates muscle tissue with randomly distributed fat. Small air bubbles may be evident in images of the RANDO® Phantom. These occur during the molding process and are small enough that they should not have a significant effect on studies.

Lung material has the same effective atomic number as the soft tissue material with a density which simulates lungs in a median respiratory state. The molded lungs are hand-shaped and fitted to naturally fill the rib cage.

Natural human skeletons are used in RANDO anthropomorphic phantoms.

IV.2.1.3 Thermoluminescence detectors

In external radiotherapy, tissue equivalent (Z_{eff}=8.18) thermoluminescence detectors (TLDs) such as TLD700(LiF: Mg, Ti) can be used for the verification of the doses delivered to the patient. In the present work *ThermoFisher* SNO78835 TLD-700 chips (3.2 x 3.2 x 0.89mm^3) were used as TLDs. For such an application, the main challenge is the establishment of the TL-dose response curve that allows the determination of the dose according to the corresponding intensity of the TL signal

IV.2.1.4 TL signal reader

In this work, the Risø National Laboratory TL/OSL-DA-20 luminescence reader was used (Fig. IV.3) [52, 53]. This reader includes three main modules:

1. Light detection system (Photomultiplier PM);
2. Stimulation system for optical and thermal light emission;
3. Additional irradiation sources: alpha, beta and X-rays.

Fig. IV.3: RISØ TL/OSL-DA20 Reader, a) The Reader, b) The Controller, c) The X-ray generator controller

The light detection system comprises a photomultiplier combined with multiple light filters. The light stimulation system includes a light emitting and heating plate source which can be used separately to make optically stimulated luminescence (OSL) or thermoluminescence TL used in this work. Additional in-situ irradiations can be provided by a beta source, an alpha source and an X-ray generator. The reader is able to analyze in a single pass 48 samples each with its own programming sequence in terms luminescence reading mode, thermoluminescence heating interval , irradiation supplementations, type of light filter, etc. The main characteristics of the used reader are summarized in table (IV.1). TLDs are placed on a stainless steel disks and exposed to X-ray or beta dose as shown on figure (IV.4).TL signal reading is performed by the same manner by just moving the disk to the reading position under the photomultiplier.

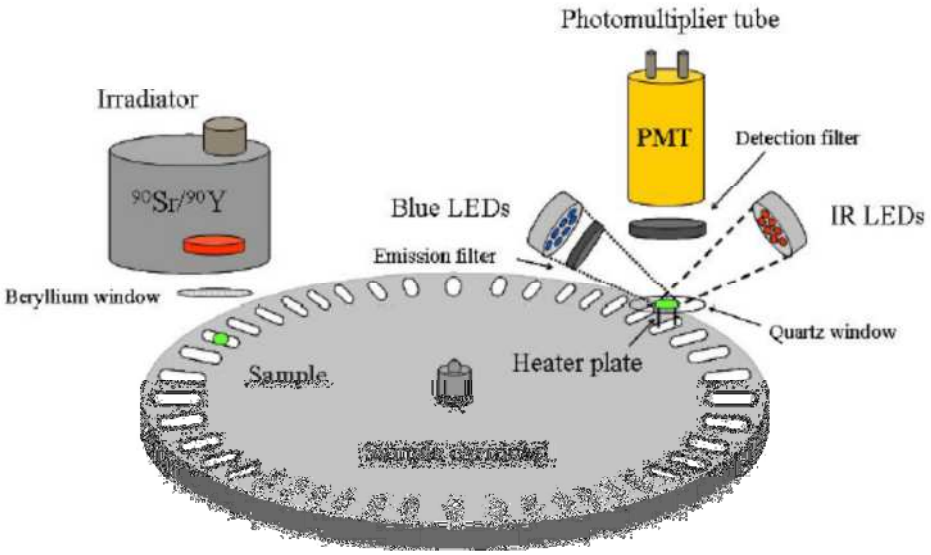

Fig. IV.4: Disks exposure and TL reading

Table IV.1: Main characteristics of RISØ TL/OSL reader

Photomultiplier	CsSbcrystal with maximum detection efficiency between 200 and 400nm and 0.4 sr as solid detection angle
Heater material	Khantal with maximal temperature of 700°C and heating rate varying from 0.1 to 10°C/s
Beta source	$^{90}Sr/^{90}Y$, Emax: 2.27 MeV, Strength: 1.48 GBq, Dose rate 0.1Gy/s in the quartz
X-ray Generator	Tungsten, 50 kV, 1 mA, 50 W, Dose rate in the quartz 2Gy/s

IV.2.1.5 Water slab Phantom

Water is the standard reference material in high energy photon dosimetry used for reference data measurement. With TLD the utilization of water phantom for dose measurement and calibration is complicated. This is why we replaced water by a polystyrene based slab RW3 phantom. Indeed, water and RW3 T29672/U5 slab phantom are used as equivalent reference media in external radiotherapy because these two materials have the same characteristics of the absorption and the scattering of the photons. RW3 is a white polystyrene material containing 2% by mass TiO2.RW3 has been developed for the use as solid water in high energy photon dosimetry (Fig. IV.5). The technical specifications of the RW3 used for calibration are presented on table (IV.2).

Fig. IV.5: RW3 slab phantom

Table IV.2: Technical specifications of the RW3 used for calibration

Device designation	RW3 slab phantom N° T29672/U5
Manufacturer	PTW-Freiburg
Intended use	Water equivalent phantom material for dosimetry in high energy photon
Material	Polystyrene (CH) containing 2% by mass titanium dioxide (TiO2)
Slab thickness	1mm, 5mm
Slab size	300mm×300mm
Density	1.045g/cm^3
Mean Z/A	0.536

IV.2.2 Experimental Procedure

IV.2.2.1 Virtual patient creation and treatment

In this work, a real patient with a lung lesion of 1394.1cm^{3}showing a similar corpulence as the Rando phantom was considered. This patient had been treated with 3D conformal radiotherapy technique at the radiotherapy centre of Setif (CLCC), Algeria. On the basis of the scanning conditions of a dedicated CT-scanner used for the patient, similar CT data were used for the Rando phantom in terms ofslice's thickness, scanning protocol and zero scanning reference (Radiological Z=0). A virtual patient was then created within the TPS by uploading the obtained CT data. On the basis of the same 3D conformal treatment technique, prescribed dose, target and organs at risk (OAR) volumes, delineation, and treatment plans of the real patient, dose calculations were performed for the virtual patient [54]. For this purpose, the corresponding real patient and Rando CT-slices were registered and fused to form resolving combined slices (images). Then, the clinician reproduced the same lesion and the structuresof the real patient on the virtual Rando patient with exactly the same positions and the same PTV. Finally, another clinician was asked to check if the same lesion was created and to perform any necessary adjustments since the anatomy of the real patient and that of the Randophantom were not exactly the same. Thus, the same delineation, beams and constraints of the real patient treatment plans, were considered as presented in Table (IV.3). On figure (IV.6) are presented: a) a 3D geometry illustration of the used treatment beams, and b) the water-equivalent RW3 slab phantoms used in this work for the dose measurements and the percent depth dose curve (PDD) comparison with the ionisation chamber.

Table IV.3: Details of the considered radiotherapy treatment plan of lung lesion. PTV – planning target volume.

Prescribed dose	40 Gy given within 20 fractions (2Gy/fraction)									
Constraint on dose	95% of the dose covers 95% of the PTV									
Number of Fields	3 with 5 segments									
Beam ID	**Technique**	**Energy(MeV)**	**Field weight**	**Gantry rotation(°)**	**Coll rotation (°)**	**Couch rotation (°)**	**Beam X (cm)**	**Beam Y (cm)**	**SSD (cm)**	**UM**
Post*	static	6X	1.084	195	0	0	14.8	15.4	87.8	97
Post.0	static	6X	0.066	195	0	0	14.8	15.4	87.8	7
Post.1	static	6X	0.076	195	0	0	14.8	15.4	87.8	7
OAD*	static	6X	0.231	300	0	0	21.4	14.8	85	23
OAD.0	static	6X	0.066	300	0	0	21.4	14.8	85	7
OAD.1	static	6X	0.072	300	0	0	21.4	14.8	85	7
ANT*	Static	6X	0.976	15	0	0	14.3	14.1	88.4	84
ANT.0	Static	6X	0.079	15	0	0	14.3	14.1	88.4	7

*Post: posterior, OAD: Oblic Anterior Right, ANT: Anterior, SSD: source to surface distance, UM: Monitor Unit.

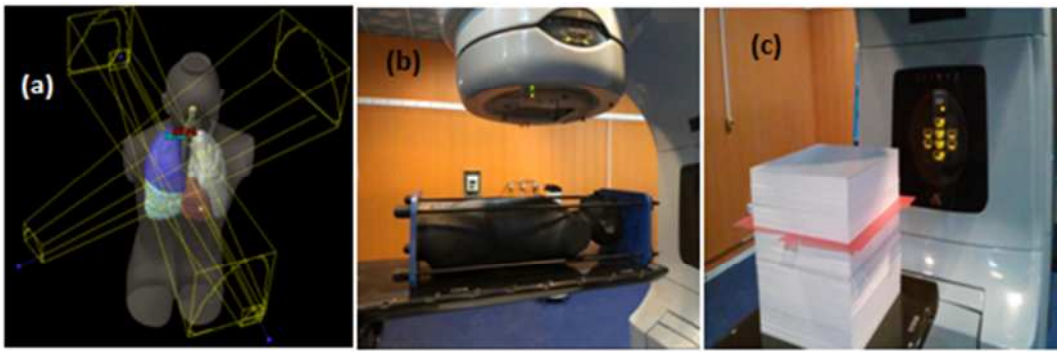

Fig IV.6: a) 3D Rando phantom image with the main treatment fields and lesion localisation (blue), b) Rando phantom placed on the radiotherapy Varian ClinacIX accelerator, c) water-equivalent RW3 slab phantoms used for TLD calibration

IV.2.2.2 TLD selection and validation before use

The signal stability (reproducibility) of the TLDs should be accessed. A general test of the reliability and stability of the detector, before using it in clinical routine, can be performed as follows. The thermoluminescence detectors are irradiated (2Gy dose), read and annealed each three times. The standard deviation of the resulting signals should be within 5%. In this work, the thermoluminescence signals were always collected under the same conditions presented in Table (IV.4) using the Risø National Laboratory TL/OSL-DA-20 luminescence reader. This procedure was performed three times. The reproducibility of the response of the TLDs was evaluated and chips with a response variation of greater than 5% were not used.

Table IV.4: Conditions of the thermoluminescence signal reading [5].

Luminescence reading mode	Thermoluminescence
Maximum reading temperature	300 °C
Heating rate	5 °C/s
TL signal sampling	250 points over the range 200 °C to 300 °C
TLD annealing conditions	10 minutes at 400°C followed by 15 minutes at 100°C

IV.2.2.3 TLD calibration

To calibrate the TLD chips the same beam quality as that used for measurements was considered. The TLD chips were first annealed at 400°C for 15 minutes followed by 300°C for 10 minutes and were left to cool down. They were then transferred to a water-equivalent RW3 slab phantom with size-adjusted inserts to house TLD chips with minimum air gap. For the determination of correction factors and the establishment of the TL-dose response curve, all TLDs were irradiatedunder reference conditions: at a *Z*-depth of 10 cm, and a given beam with a field size of $10x10cm^2$ and isocentric SAD-set-up (source-axis distance of 100 cm) (Fig. IV.7). Thus, all TLDs were given a dose of 2Gy for the determination of the correction factors.

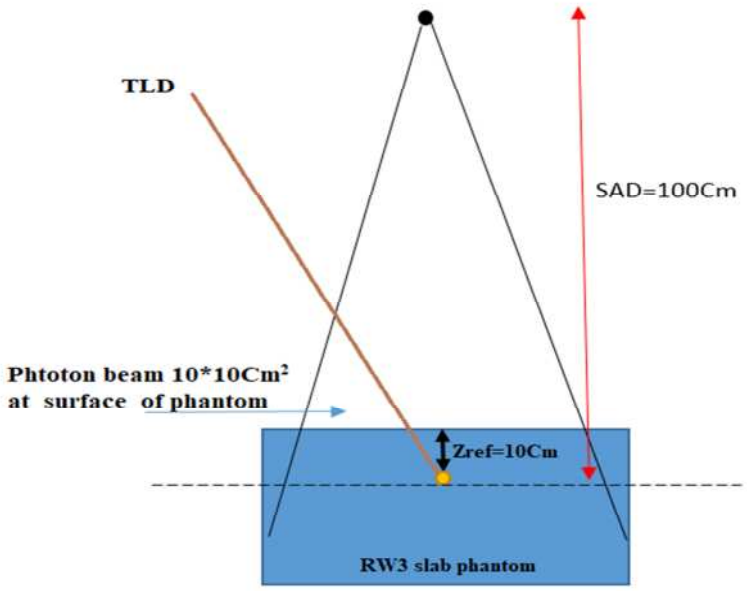

Fig. IV.7: TLD calibration setup under reference conditions

The measured TL signal to be used for dose determination must be corrected according to Equation (IV.1). Thus, four correction factors were considered for optimal accuracy. These correction factors are given by the following equations Eq. IV.2 - element correction factor $\boldsymbol{E_i}$ for each used TLD, Eq.IV.3 - actual to reference TL measurement ratio $\boldsymbol{R}$ for a dose of 2Gy, Eq.IV.4 - TLD weight correction factor $\boldsymbol{W_i}$, and Eq.IV.5 - Riso OSL/TL reading position and calibration correction factor $\boldsymbol{P_i}$.

$$TL_{corr} = TL_{meas}.R.E_i.W_i.P_i \quad \text{(IV.1)}$$

$$E_i = \frac{TL_{mean}}{TL_i} \quad \text{(IV.2)}$$

$$R = \frac{TL_{act}(2Gy)}{TL_{ref}(2Gy)} \quad \text{(IV.3)}$$

$$W_i = \frac{m_i}{m_{mean}} \quad \text{(IV.4)}$$

$$P_i = \frac{TL(P_i)}{TL_{mean}(allpositions)} \quad \text{(IV.5)}$$

Where TL_{corr} is the corrected TL intensity, TL_{meas} is the measured TL intensity (integral value), TL_{mean} is the mean TL intensity of all TLDs measured at 2 Gy dose, TL_i is the TL intensity of a given TLD measured at 2 Gy, TL_{act} is the measured TL intensity of the reference TLD for the actual experiment and a dose of 2 Gy, TL_{ref} is the measured TL intensity of the

reference TLD for the first calibration experiment (reference) and a dose of 2 Gy, m_i is the TLD weight, m_{mean} is the average weight of all TLDs, $TL(P_i)$ is the measured TL intensity of the reference TLD at any given TL reading position in the reader for a dose of 2 Gy, $TL_{mean}(all\ positions)$ is the mean TL intensities of the reference TLD for all TL reading positions of the reader and a dose of 2 Gy.

IV.2.2.4 Dose response curve

The TL dose response curve was established by measuring the TL signal intensities corresponding to the following doses: 0.1, 0.5, 1, 1.5, 2 and 2.5 Gy. The used TLDs were all irradiated at reference TPS conditions using the water-equivalent RW3 slab phantoms. The irradiation was performed with the same treatment photon energy (at 6MV) which is delivered by the Varian ClinacIX accelerator. The TLDs were read just after exposure to the planned doses.

IV.2.2.5 Percent Depth dose checking

As it is well known, the PDD is a very important measure of clinical beam data for dose calculation. To check if the used TLDs gives a correct response when considering in-depth dose measurement as it is in this work. At the CLCC radiotherapy service, this curve is established and routinely checked using a calibrated PTW 31010 - 0.125cc Semiflex ionisation chamber and a water phantom. In order to verify the ability of the used TLDs to reproduce the same PDD as that obtained with the ionisation chamber, the main doses of the PDD were measured by TLDs using suitable water-equivalent RW3 slab phantoms. Thus, dose were checked at three depth position: surface, build-up position (1.5 cm), and at TPS reference depth (10 cm). For this verification a standard field of $10x10cm^2$ with a source-to-surface distance (SSD) of 100cm and photon energy of 6MeV were considered.

IV.2.2.6 TLD Dose measurements on Rando phantom

In this work, 19 dose-measurement positions were carefully selected within the Rando phantom on the basis of the CT data as presented in figure (IV. 8).According to the available holes in the Rando phantom, the locations of the dosimeters were selected to cover the PTV, the OARs such as heart and spinal cord, and the heterogonous tissue interfaces from both sides. Then the beams listed in Table (IV.3) were delivered to the RANDO phantom according to the radiotherapy treatment plan, and the dose was measured at the various

selected points using TLDs. TLD irradiation, reading, and annealing were performed following the same protocol used for their calibration.

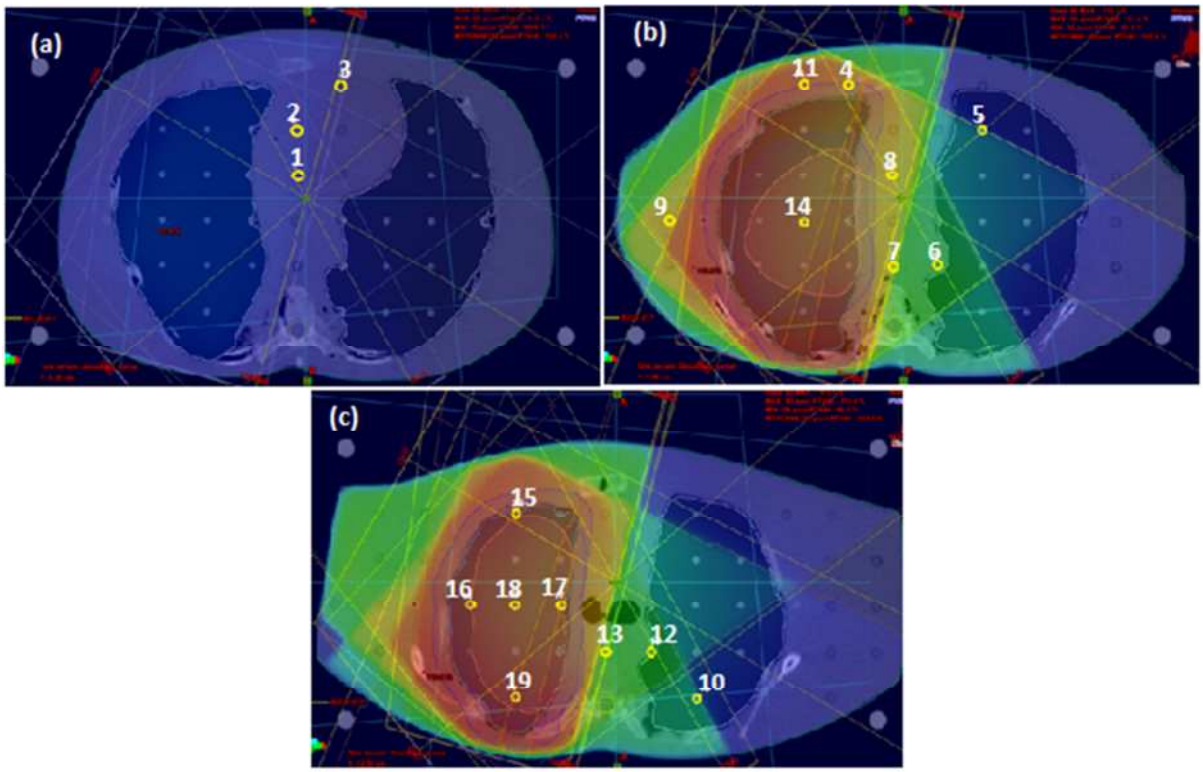

Fig. IV.8: TLD positions shown on CT-sliceswith radiotherapy beams angles: (a) slice with y=6.3cm, (b) slice with y=9cm, (c) slice with y=12.3 cm.

IV.2.2.7 Dose calculation and heterogeneity correction

In this work, dose calculation was performed by the beamlets convolution/superposition anisotropic analytical algorithm (AAA) version 11.0.31 implemented in the Varian Eclipse TPS. Configuration of the AAA is based on basic physical parameters determined by means of Monte Carlo simulation, where the parameters were adapted to measured clinical beam data. The AAA algorithm included the Monte Carlo simulation of the primary photons, the scattered and extra-focal photons and the scattered electrons. Heterogeneity correction was performed at three levels: transversally, laterally and at the heterogeneous tissue interfaces such as soft tissue-lung and soft tissue-bone. Corrections were made on the basis of Eqs. (IV.6), (IV.7), and (IV.8) [8]. Moreover, AAA has a different approach of accounting for

heterogeneities compared with other algorithms which depend on the type of the heterogeneity considered (air, bone...), tissue density and tumour location [55-57].

$$I_\beta(Z,\rho) = I_\beta\left(\grave{Z}\right), with\ \grave{Z} = \int_0^Z \frac{\rho(t)}{\rho_{water}} dt \quad \text{(IV.6)}$$

$$K_\beta\left(x_\beta, y_\beta, z_\beta\right) = \frac{\rho(x,y,z)}{\rho_{water}} \sum_{k=0}^{5} c_k\,(\grave{z}) \frac{1}{r} e^{-\mu_k r_d(x,y,\rho)},\ with r_d(x,y,\rho) = \int \frac{\rho(\vec{t})}{\rho_{water}} d\,\vec{t} \quad \text{(IV.7)}$$

$$k_z(z) = \frac{\rho(z)}{\rho_{water}(z)} \sum_{i=1}^{2} c_i \frac{1}{\mu_i} e^{-\mu_i \grave{z}} \quad \text{(IV.8)}$$

Where: $I_\beta(Z,\rho)$ is the energy deposition function considering heterogeneities, Z is the depth of calculation point,$\grave{Z}$is the radiologic distance from the Kernel origin, $\rho(t)$is the mass density of the tissue, ρ_{water} is the water density, $K_\beta(x_\beta,y_\beta,z_\beta)$ is the diffusion kernel at the beamlet coordinates$(x_\beta,y_\beta,z_\beta)$, c_k is the kernel weighting factor allowing the normalization of the total kernel energy, μ_k is the attenuation constant, r_d is the radiologic distance from the depth Z which is the origin from the kernel point to the point of coordinates (x,y,z), $\vec{t}$ is the integral line from the kernel origin (0,0,z) to (x,y,z), k_z is the one dimensional 1D diffusion kernel, c_i and μ_i are coefficients determined by Monte-Carlo kernels of each beamlet.

IV.3 Results and Discussion

IV.3.1 TLD section and validation before use

After being properly annealed and to check the reproducibility of the detectors the TLDs were irradiated three times by the Varian VF-50JX-ray tube (50KV, 1mA) and given a dse of 2Gy. The calculation of the percent standard deviation is used to assess the reproducibility (Table IV.5).

$$\%SD = \frac{SD}{TL_{mean}}.100 \quad \text{(IV.9)}$$

With: SD is the standard deviation and TL_{mean} is the mean TL value.

Table IV.5: Results of TLD selection

TLD N°	TL max	Standard deviation (SD)	Percentage SD (%)
1	1227	2.49	0.20
	1225		
	1231		
2	789	1.67	0.21
	793		
	790		
3	827	2.16	0.26
	826		
	831		
4	1077	5.44	0.5
	1090		
	1081		
5	1076	7.48	0.69
	1082		
	1094		
6	1124	12.19	1.07
	1147		
	1152		
7	1225	14.16	1.15
	1248		
	1214		
8	1061	12.36	1.16
	1085		
	1057		
9	1060	17.44	1.63
	1060		
	1097		
10	1026	17.44	1.68
	1063		
	1092		
11	619	10.62	1.68
	633		
	645		
12	1149	21.27	1.8
	1192		
	1196		
13	1111	20.24	1.87
	1080		
	1062		
14	1307	27.21	2.03
	1348		
	1373		
15	1152	23.25	2.07
	1096		
	1115		
16	1002	24.25	2.34
	1059		
	1045		
17	1139	31.97	2.82
	1094		

	1172		
18	1121	55.37	1.53
	1156		
	-		
19	1154	77.467	0.51
	1166		
	-		

TLDs with standard deviation more than 5% are rejected and excluded from the use in this study.

IV.3.2 TLD calibration

All TLDs were placed in RW3 slab phantom and all given a dose of 2Gy with the Linac using photons E=6MV under reference conditions (SAD setup).The correction factors were established for the same beam quality used for treatment for each TLD and are shown in the Table (IV.6) below:

Table IV.6: TLDs calibration and correction factors.

TLD N°	**Weight (mg)**	***Wi***	***Pi***	***Ei***
1	23.8	0.98604	0.65173	0.93933
2	24.3	1.00676	0.55047	0.93995
3	24.3	1.00676	0.77869	0.87079
4	23.4	0.96947	0.67018	0.96374
5	24.3	1.00676	0.89727	0.9095
6	24.4	1.0109	0.84006	0.9597
7	24.2	1.00262	0.62506	0.84678
8	24.1	0.99847	1.11205	1.12235
9	23.9	0.99019	0.76485	0.90045
10	23.9	0.99019	1.25362	0.72552
11	24.5	1.01505	1.00082	1.08129
12	24.4	1.0109	0.64525	0.78995
13	24.4	1.0109	0.72134	0.93118
14	24.1	0.99847	1.03908	0.99817
15	24.3	1.00676	0.99197	0.99001
16	23.0	0.9529	1.23332	1.47829
17	24.4	1.0109	0.98124	1.05702
18ref	24.7	1.02333	0.93097	1.57761
19	24.2	1.00262	0.94477	0.91836

IV.3.3 Dose response curve establishment

The results of the obtained TL signals (glow curves) after all TLDs irradiation to different doses are shown in Fig (IV.9).

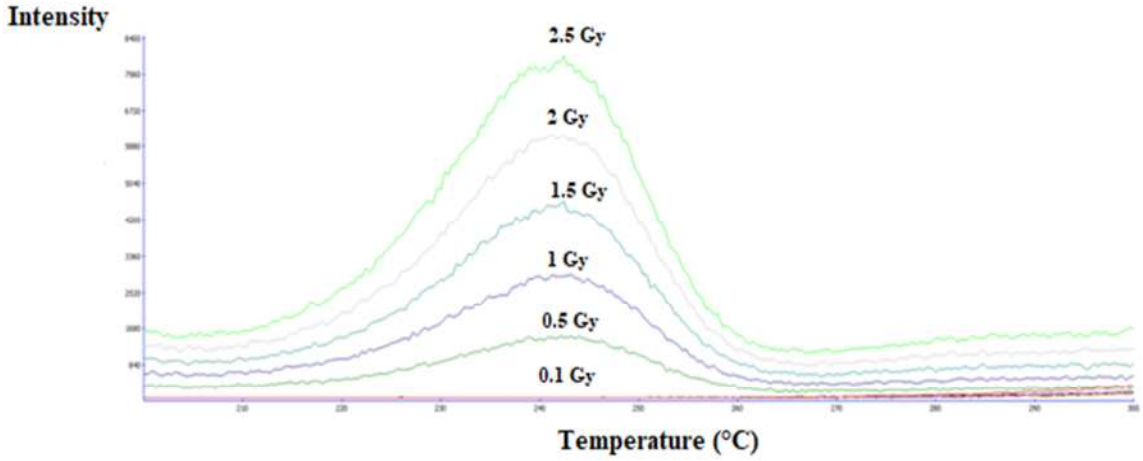

Fig.IV.9: Obtained TL signals for dose response established of the reference TLD.

Thus, the TL dose response curve (*TL=f(D)*) was established by measuring the TL signal intensities corresponding to the following doses: 0.1, 0.5, 1, 1.5, 2 and 2.5 Gy. The TL intensities are shown on table (IV.7).

Table IV.7: TL intensities corresponding to different irradiation doses.

TLD N°	Dose (Gy)	Corresponding monitor units UM	TL Integral
6	0.1	13	8363
8	0.5	63	31865
11	1	125	73700
16	1.5	188	92977
18	2	251	143650
17	2.5	313	167152

Results of table (IV.7) are plotted on the graph of figure (IV.10). It can be easily verified that the response of the TLDs is quiet linear along the considered dose-interval. The linear fit of

the experimental data allowed determination of an experimental relation (Eq. (IV.10)) which was used for accurate dose determination in Gray (Gy) from any measured TL intensity.

$$\boldsymbol{TL} = (64500 \pm 1300) * \boldsymbol{D} + (1800 \pm 380) \qquad \text{(IV.10)}$$

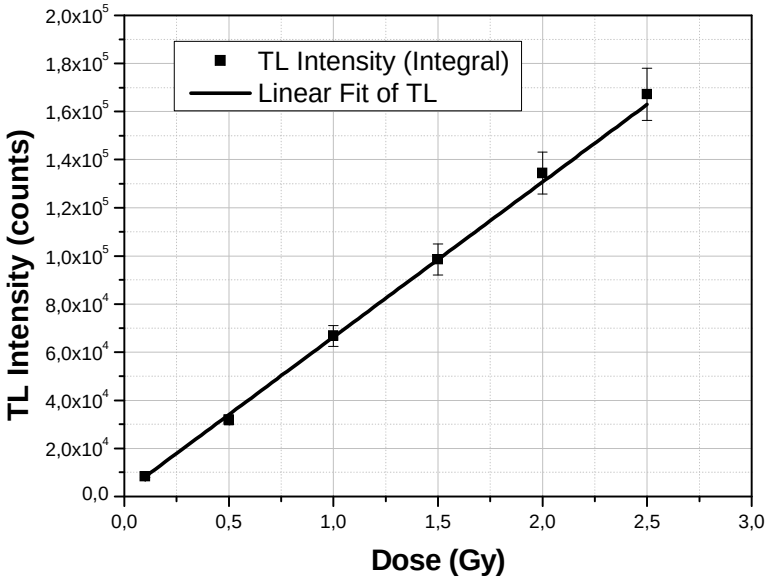

Fig IV.10*:* TL-dose response curve.

IV.3.4 Percent depth dose (PDD) checking

The TL signals obtained after the TLD exposition at the three considered depths are presented in figure (IV.11).

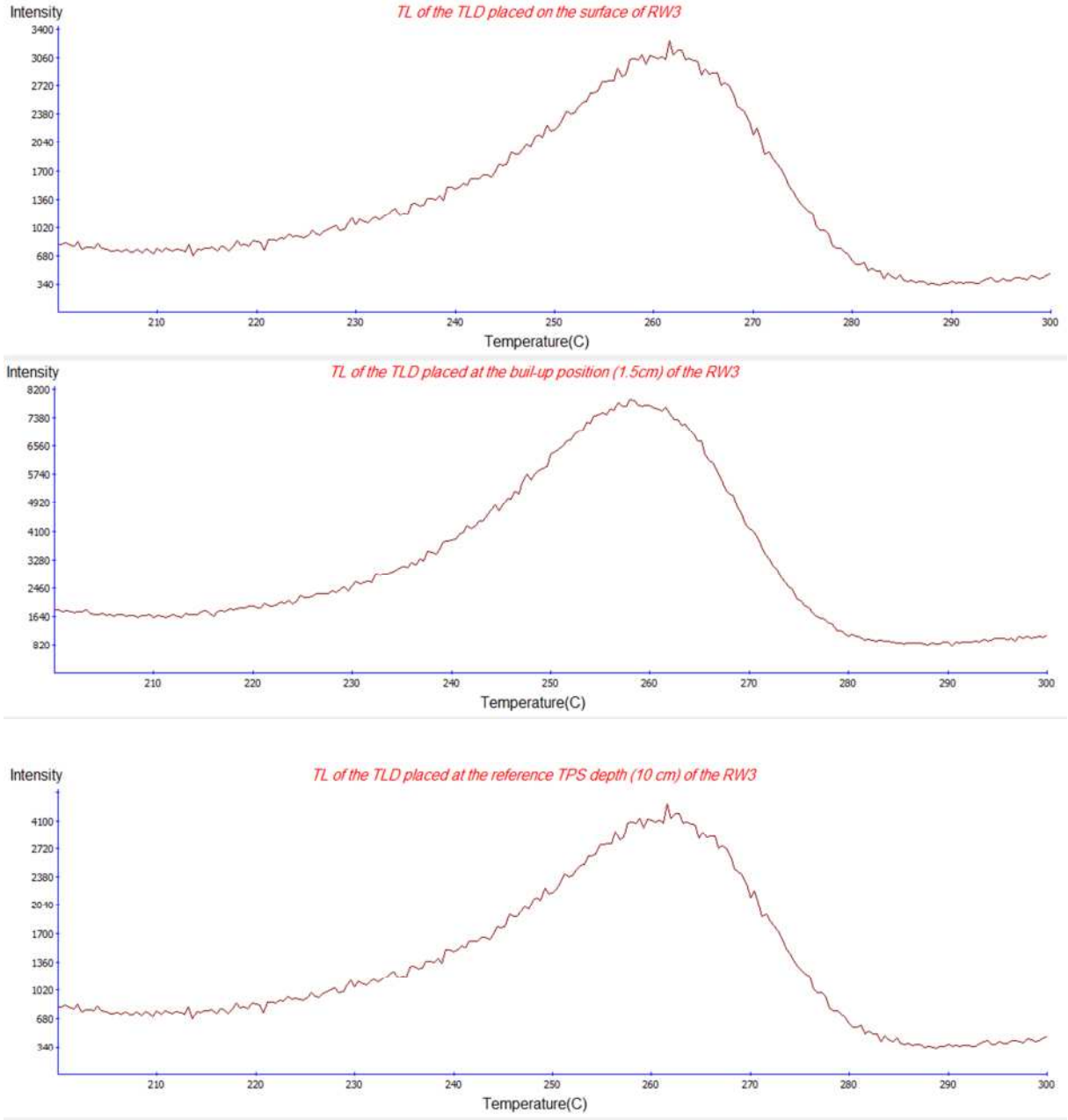

Fig. IV.11: Obtained TL signal for PDD checking.

The irradiation conditions and the obtained doses after TLD reading are shown on table (IV.8). The comparison between depth dose curves measured by the routinely used calibrated ionisation chamber and by the TLDs demonstrates that the TLDs were able to reproduce an accurate PDD (Fig. IV.12).

Table IV.8: PPD results obtained by TLD

TLD N°	UM	Depth of irradiation	Dose (Gy)	% Value
18	949	Z=0 cm surface	2.05	52.66
18	949	Z=1.5cm buil-up	4	100
18	949	Z=10 cm (reference)	2.5	67.37

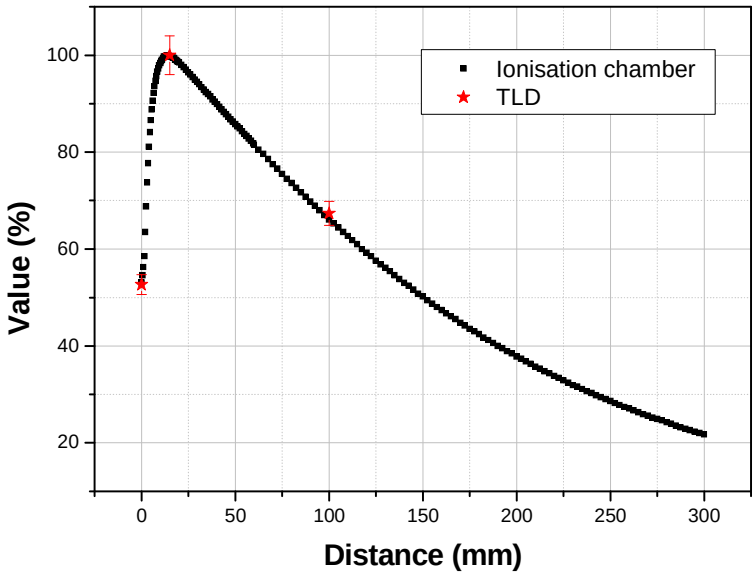

Fig.IV.12: Central axis percent depth dose (PDD) as measured by means of an ionisation chamber and the thermoluminescence dosimeters (TLDs) in water and water-equivalent RW3 slab phantoms for a 6 MV photon beam of a field size of 10×10 cm^2. Measured doses are normalized to the dose at a depth of 1.5 cm (build-up Z_{max})

IV.3.5 Comparison between calculated and measured doses

Results of TLD doses measured at various depths within the Rando phantom are shown in Table (IV.9) and compared to the doses calculated with the AAA with and without heterogeneity correction. Additionally, the difference between the calculated corrected dose and the measured dose is also shown.

Table IV.9: Different AAA-calculated (AAA: anisotropic analytical algorithm) and TL-measured (TL: thermoluminescence) doses and differences Δ of HC-doses to without-HC doses and TL-measured doses to reference HC-doses. HC – heterogeneity correction; WHC – with heterogeneity correction; WOHC – without heterogeneity correction; see Fig (IV.8) for location of TLDs; grey: positions at lung interfaces

TLD location	**Calculated Dose** Without HC (D_{WOHC}) (Gy)	**Calculated Dose** With HC (D_{WHC}) (Gy)	**Δ(%)** $\frac{D_{WHC}-D_{WOHC}}{D_{WHC}}.100$	**Measured Dose** (D_{TL}) (Gy)	**Δ(%)** $\left\lvert\frac{D_{TL}-D_{WHC}}{D_{TL}}.100\right\rvert$
1	0.097	0.087	-11,50	0.094±0.004	7.45
2	0.27	0.25	-8.00	0.27±0.01	7.41
3	0.24	0.21	-14,29	0.23±0.01	8.70
4	1.90	2.11	9,95	2.08±0.10	1.44
5	0.20	0.17	-17,65	0.18±0.015	5.56
6	0.28	0.28	0.00	0.32±0.02	**12.50**
7	1.28	1.05	-21,90	1.04±0.05	0.96
8	1.81	1.71	-5,85	1.70±0.08	0.59
9	0.60	0.54	-11,10	0.52±0.06	3.85
10	0.19	0.27	29,63	0.29±0.01	6.90
11	1.96	2.13	7,98	2.17±0.10	1.84
12	0.27	0.21	-28,58	0.24±0.01	**12.50**
13	0.55	0.51	-7,84	0.51±0.02	0.00
14	1.95	2.09	6,70	2.08±0.10	0.48
15	1.99	2.10	5,24	2.23±0.10	**5.82**
16	2.09	2.03	-2,95	2.04±0.10	0.49
17	1.99	2.01	1.00	2.00±0.10	0.5
18(ref.)	2.01	2.07	2,90	2.09±0.10	0.96
19	2.16	2.09	-3,35	2.13±0.10	1.88

TL-measured doses at the lung interfaces (TLD N° 6, 12 and 15) demonstrate a high difference (Δ) to the corrected doses. This is maybe due to some limitation of the used algorithm to well predict the build-up of dose near tissue interfaces broadening the lungs. Thus, in case of a strong heterogeneity, AAA dose correction is very significant. Indeed, the average Δ difference between calculated and measured doses for a low dose range (<0.5Gy) is

about 6.5% and while it is about 1.0% for a higher dose range (>0.5Gy). It is also confirmed that the maximum total dose measured by the TLDs in the heart does not exceed the value of 5.4Gy (Position 2), a value which is below the OAR constraints considered in the actual radiotherapy plan. It was also found that the measured doses within the PTV were consistent with the ICRU recommendations. All the corrected calculated doses and measured doses of the PTV (Table IV.9) were found to be in the interval of 95%-107% (1.9-2.14Gy) of the prescribed dose (2Gy) except for positions 11 and 15 where the measured doses were found relatively outside this interval. These results and findings confirm that an adequate dose delivery to the PTV is possible with the considered treatment plans validated during the TPS calculation phase and actually used. This treatment plans can be improved if more attention is paid to the interface and near interface areas such as positions 15 and 11. The CLCC radiotherapy service was also advised to implement the intensity modulation radiotherapy (IMRT) which can help to overcome such point-doses problems better than conformal technique with the used heterogeniety correction algorithm.

IV.3.6 Heterogeneity effect on calculated doses

The present results indicate that tissue heterogeneity is an important aspect that needs to be considered for dose optimization of the treatment plans. Therefore, the calculated dose distribution with and without heterogeneity correction as well as the TL-measured doses were compared to the prescribed dose. The exact coordinates of the TLDs positions, the corresponding Hounsfield units (HU), and the percentage (%) of the calculated and measured doses with respect to the prescribed dose (2Gy) for the above mentioned situations are presented in Table (IV.10). On this table we can check the conformity of local point-dose with already mentioned recommendations and if there any hot point dose.

Table IV.10: Percentage (%) of the heterogeneity correction (HC) doses, without HC doses, and TL-measured doses with respect to the prescribed dose (2Gy). PTV – planning treatment volume; HU – Hounsfield unit; TLD – thermoluminescence dosimeter; GTV- Gross tumour volume, see Fig (IV.8) for location of TLDs.

TLD location	**Coordinates (cm)**			**HU_{av} (Location)**	**% of the dose without HC toprescribed dose**	**% of the dose with HC toprescribed dose**	**% of the measured TL dose toprescribed dose**
	X	Y	Z				

1	2.52	6.3	1.62	17.75(Heart)	4.9	4.4	4.7
2	-0.50	6.3	4.64	19.75(Heart)	13.5	12.5	13.5
3	-0.54	6.3	7.59	13.25(Heart)	12.0	10.5	11.5
4	-3.65	9	7.57	25.75(Soft tissue, GTV)	95.0	105.5	104.0
5	5.44	9	4.49	-669(Lung L)	10.0	85.0	9.0
6	2.44	9	-4.53	**10.5/-650*** (Interface)	14.0	14.0	16.0
7	-0.57	9	-4.53	12.75(Soft tissue)	64.0	52.5	52.0
8	-0.57	9	1.52	13.75(Soft tissue)	90.5	85.5	85.0
9	-15.67	9	-1.34	12.5(Soft tissue)	30.0	27.0	26.0
10	5.36	12.3	-7.67	-476.25(Lung L)	9.5	13.5	14.5
11	-6.58	9	7.61	12(Soft tissue, GTV)	98.0	106.5	108.5
12	2.41	12.3	-4.54	**20/-433.5*** (Interface)	13.5	10.5	12.0
13	-0.65	12.3	-4.46	22.5(Soft Tissue)	27.5	25.5	25.5
14	-6.62	9	-1.45	-469(Lung L, PTV)	97.5	104.5	104.0
15	-6.65	12.3	4.56	**8/-705.75*** (Interface)	99.5	105.5	111.5
16	-9.64	12.3	-1.55	-439.25(Lung L, PTV)	104.5	101.5	102.0
17	-3.63	12.3	-1.51	-404(Lung L, PTV)	99.5	100.5	100.0
18	-6.65	12.3	-1.51	-434.25(Lung L, PTV)	100.5	103.5	104.5
19	-6.69	12.3	-7.56	-339.5(Lung L, PTV)	108.0	104.5	106.5

*HUs ofsoft tissue/lung interface.

In this study, the shape differences of the dose-volume histograms (DVHs) were also evaluated for the main structures and volumes with and without heterogeneity correction. Indeed, DVH is an important tool to evaluate the performance of the heterogeneity correction algorithm and to verify if the major constraints on dose delivery are respected or not. Analysing the DVHs it could be verified that the used algorithm is very effective to generally address the problem of dose delivery in case of heterogeneities. It could also be checked that the PTV planed dose and the OAR dose constraints were generally respected (Fig. IV.13). Figure (IV.13) shows that, after correction, the PTV volume is well covered and the delivered dose is within the interval recommended by the ICRU50. Moreover, the OARs dose-constraints are also well respected.

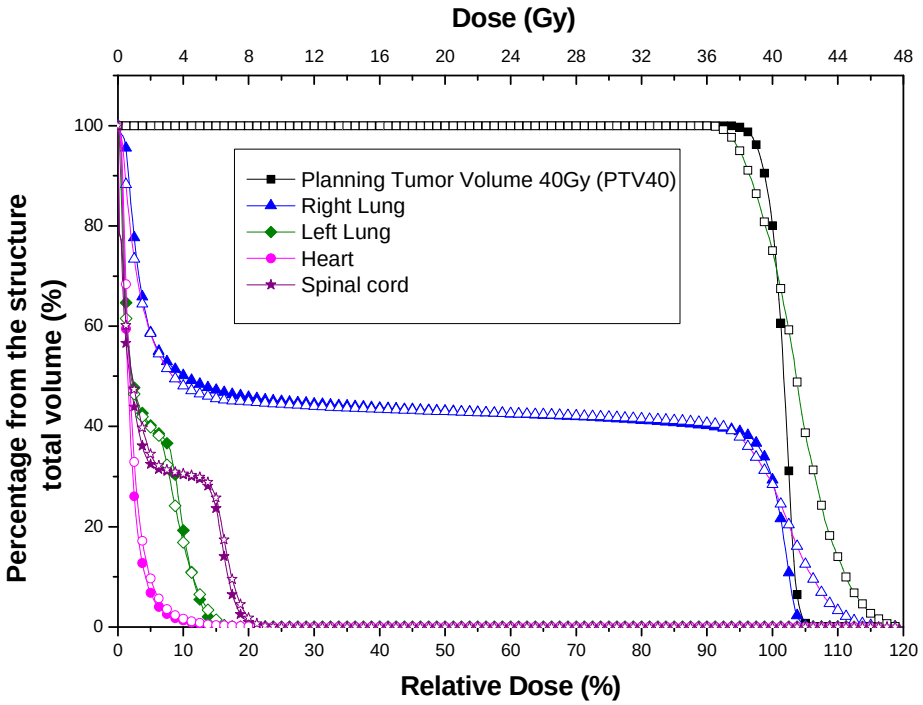

Fig.IV.13: Dose-volume histograms (DVHs) with heterogeneity correction (solid symbols) and without heterogeneity correction (Open symbols) calculated for the most important organs and volumes

Although the constraints on dose delivery were generally respected after heterogeneity correction, the comparison of the same point-doses between heterogeneity-corrected plans and the non-corrected plans (Table IV.9) demonstrates that the minimum (diminution), the mean, and the maximum (augmentation) dose differences are -28.58%, -3.66%, and 29.63%, respectively. The largest source of error in the calculations exists in heterogeneous tissue such as left lung in positions 5, 10 and 12, and spine in position 7. Thus, it is demonstrated that the presence of large heterogeneities cannot be entirely accounted for by the AAA algorithm when compared to dosimetry-measurements, especially in lower-dose areas such as heart, spine and left lung and for heterogeneous interfaces. We found a borderline of 13% in terms of calculated dose difference on the horizontal segment distant from z=-6.7 cm to z=-7.8cm (x=0cm and y=9cm) to the left of the PTV limit inside the spine.

Finally, it should be mentioned that the algorithms for heterogeneity correction are classified by the task group 65 (TG-65) of the Radiation Therapy Committee of the American Association of Physicists in Medicine [58] into categories from 1 to 4 according to the level of anatomy sampled for the scatter calculation and the inclusion or exclusion of electron

transport. The 3D AAA algorithm used in the present study is classified as a category 4. In a study using a Rando phantom, Bragg and Conway reported that the difference between the dose calculated using the AAA algorithm and the dose measured experimentally was within 2.5% or 2 mm in the presence of heterogeneity [59]. Ronde and Hoffmann demonstrated that the dose deviation in lung lesions using AAA was less than 3% for most treatment plans [60]. The TG-65 recommends that a category 4 algorithm must be considered in order to quantify the dose at tumor/lung interfaces in radiation planning for the lung and that one-dimensional correction are reasonable only for point dose estimates for lung tumors. Kry et al. compared many algorithms used for heterogeneous dose calculations and stated that all algorithms (AAA, Pinn, Xio, Tomo and PB) except Monte Carlo (MC) overestimated the dose that was delivered to a lung tumor at the center (not at the interface or periphery) by 3.9% on average [61]. Ottosson et al. observed dose deviations of less than 1% for isocentric field techniques centered in the middle of a heterogeneous phantom, whereas dose deviations of more than 4% were observed for some laterally shifted treatment plans [62]. Finally, attention must be paid to the new technical aspects of in-vivo dosimetry and lung radiation therapy techniques with the focus on dosimetry applications using imaging devices [63].

Conclusions

In this work it was question to evaluate the performance of the Varian-Eclipse TPS used by the CLCC in terms of dose calculation accuracy. The evaluation was regarding the application of 3D conformational radiotherapy and by considering tissue heterogeneities that constitute real and complicated cases for accurate dose calculation. The results of the experimental part presented in this work indicate that TLDs can be used for point dose measurements in order to check the TPS-calculated dose, particularly, for cases presenting tissue heterogeneity. Indeed, the shape of the PDD curve obtained using TLDs was found in very good agreement with that obtained with a calibrated ionisation chamber. This confirms that TLD's allow measurement of point dose at different depths. Close attention should be paid to use of the Varian Eclipse TPS with its heterogeneity correction algorithm (AAA) for dose calculations involving heterogeneities of low-density media. In the case studied here, lower deviations between TLD-measured and calculated doses were observed in homogenous media. The results of TL point-dose measurements are generally in good agreement with the calculated doses. However, close to the heterogeneity interfaces, results show some relatively high deviations between calculated and measured doses although it was found that for the worst case, the constraints on PTV and OARs dose delivery are well respected. Thus, the AAA algorithm is more accurate for dose calculation in treating deep-seated tumours beyond heterogeneity interfaces. It is, therefore, recommended that the algorithm used for the heterogeneity correction must be continuously improved by studying and reporting all specific cases where the algorithm fails. Physicists should also well understand the effect of the correction algorithm on calculated dose and maintain an open dialogue with clinicians on some specific cases of tissue heterogeneity. In conclusion, although the measured doses are in good agreement with the calculated doses in major tissues, it should be kept in mind that there may be discrepancies between the calculated dose and the real delivered dose in heterogeneous media.

References

[1] Bodry JM (2009), *La dosimétrie externe des rayonnements ionisants de la référence nationale aux utilisateurs en radiothérapie et en radioprotection*, Rapport CEA-R-6214.

[2] Van Dam J, MarinelloG (2006), *Methods for in vivo dosimetry in external radiotherapy*, ESTRO Mounierlaan 83/12 – 1200, Brussels.

[3] Wesolowska PE, Cole A, Santos T, Bokulic T, Kazantsev P, Izewska J (2017), *Characterization of three solid state dosimetry systems for use in high energy photon dosimetry audits in radiotherapy*, Radiation Measurements. 106, 556-562.

[4] Bøtter-Jensen L (2000), *Development of Optically Stimulated Luminescence Techniques using Natural Minerals and Ceramics, and their Application to Retrospective Dosimetry*. Risø National Laboratory, Roskilde.

[5] Furetta C (2003), *Handbook of Thermoluminescence*, World Scientific Publishing, London.

[6] Oberhofer M, Scharmann A (1979) Eds. *Applied thermoluminescence dosimetry*. Bristol: Adam Hilger.

[7] Varian (2010), *Eclipse Algorithm Reference Guide*. P/N B502679R03B.

[8] Varian (2009), *Varian medical system :manuel de référence des algorithms Eclipse*, v.P/N B502612R03A.

[9] Landberg T, Chavaudra J, Dobbs J, Hanks G, Johansson KA (1993), *Report 50: Prescribing, Recording and Reporting Photon Beam Therapy*. Journal of the International Commission on Radiation Units and Measurements (ICRU), 26 (1).

[10] Landberg T, Chavaudra J, Dobbs J, Gerard JP, Hanks G, Horiot JG, Johansson KA, Möller T, Purdy J, Suntharalingam N, Svensson H (1999), *Report 62: Prescribing, Recording and Reporting Photon Beam Therapy (Supplement to ICRU report 50).Journal of the International Commission on Radiation Units and Measurements (ICRU)*, 32 (1).

[11] Khan M F, *The Physics of Radiation Therapy*, 2nd edition, (Lippincott Williams & Wilkins, 1994, USA).

[12] Reports No. 103, *AAPM Task Group 103 report on peer review in clinical radiation oncology physics*, Journal of Applied Clinical Medical Physics, Vol. 6, Issue 4 http://www.aapm.org/pubs/reports/RPT_103.pdf.

[13] *Radiation Oncology Physics Handbook*. Ervin Podgorsak, Editor. http://www-naweb.iaea.org/nahu/dmrp/syllabus.shtm

[14] JV Dyk, RB Barnett and JJ Battista, *Computerized Radiation Treatment Planning Systems*, in : Modern technology of radiation oncology, Medical Physics Publishing. http://www.medicalphysics.org/apps/medicalphysicsedit/VANDYKCH08.pdf

[15] F. Hasenbalg, H. Neuenschwander, R. Mini, E.J. Born . *Collapsed cone convolution and analytical anisotropic algorithm dose calculations compared to VMC++ Monte Carlo simulations in clinical cases*. Phys Med Biol, 52:3679-36691, 2007.

[16] A. Gray, L.D. Oliver, P.N. Johnston. *The accuracy of the pencil beam convolution and anisotropic analytical algorithms in predicting the dose effects due to attenuation from immobilization devices and large air gaps*. Med. Phys., 36:3181-3191, 2009.

[17] Y. A. Hu, H. Song, Z. Chen, S. Zhou S, F.F. Yin. *Evaluation of an electron Monte Carlo dose calculation algorithm for electron beam*. J Appl Clin Med Phys, 9:2720, 2008.

[18] P.S. Kroon, S. Hol, M. Essers, *Dosimetric accuracy and clinical quality of Acuros XB and AAA dose calculation algorithm for ste-reotactic and conventional lung volumetric modulated arc therapy plans*, Radiat Oncol, 8:149, 2013.

[19] T. Han, J.K. Mikell, M. Salehpour, F. Mourtada, *Dosimetric comparison of Acuros XB deterministic radiation transport method with Monte Carlo and model-based convolution methods in heterogeneous media*, Med Phys 38:2651-2664, 2011.

[20] S. Rana, K. Rogers, T. Lee, D. Reed, C. Biggs, *Verification and Dosimetric Impact of Acuros XB Algorithm for Stereotactic Body Radiation Therapy (SBRT) and RapidArc Planning for Non-Small-Cell Lung Cancer (NSCLC) Patients*, Int J Med Phys Clin Eng Radiat Onc, l2:6-14, 2013.

[21] D.P Huyskens, R. Bogaets, J. Verstraete, *Practical guidelines for the implementation of in vivo dosimetry with diodes in external radiotherapy with photon beams (entrance dose)*, 2001-First edition by European Society for Therapetic Radiology and Oncology (ESTRO), booklet n°5.

[22] Muhammad Maqbool, *An Introduction to Medical Physics*, Springer, 2017.

[23] B. Emami, *Tolerance of Normal Tissue to Therapeutic Radiation, Reports of Radiotherapy and Oncology*, Vol.1, N°1, Department of Radiation Oncology, Loyola University Medical Center, Maywood, Illinois, USA, 2013.

[24] J.K. Annkah et al., *Assessment of the dosimetric accuracies of CATPhan 504 and CIRS 062 using kV-CBCT for performing direct calculations*, Journal of Medical Physics, Vol. 39, No. 3, 133-41, 2014.

[25] F. Tatsugami et al., *Electron density and effective atomic number images generated by dual energy imaging with a 320-detector CT system: A feasibility study*, European Society of Radiology, ECR 2014, DOI:10.1594/ecr2014/C-0403

[26] R. Suresh, *Verification and dosimetric impact of Acuros XB Algorithm for Stereotactic Body Radiation Therapy (SBRT) and RapidArc planning for Non-Small-Cell Lung Cancer (NSCLC) patients*, International Journal of Medical Physics, Clinical Engineering and Radiation Oncology, 2(1):6-14, 2013.

[27] L.A.R. da Rosa et al., *Percentage depth dose evaluation in heterogeneous media using thermoluminescent dosimetry*, Journal of Applied Clinical Medical Physics, Vol.11, N°1, 2010

[28] H. F. Batho, *Lung corrections in cobalt 60 beam therapy*, J. Can. Assoc. Radiol. 15:79–83, 1964.

[29] M. R. Sontag and J. R. Cunningham, Corrections to absorbed dose calculations for tissue inhomogeneities, Med. Phys. 4:431–436, 1977.

[30] U. Fano, *Note on the Bragg-Gray cavity principle for measuring energy dissipation*, Radiat. Res. 1:237–40, 1954.

[31] J. E. O'Connor, *The variation of scattered x-rays with density in an irradiated body*, Phys. Med. Biol. 1:352–69, 1957.

[32] A. Ahnesj, M.M. Aspradakis, *Dose calculations for external photon beams in radiotherapy*, Phys. Med. Biol. 44 R99–R155, 1999.

[33] P.W0 Hoban, D.C. Murray, W.H. Round, *Photon beam convolution using polyenergetic energy deposition Kernels*, Phys. Med. Biol. **39** 669–85, 1994

[34] N. Papanikolaou et al., tissue inhomogeneity corrections for megavoltage photon beams, Report of Task Group No. 65 of the Radiation Therapy Committee of the American Association of Physicists in Medicine, 2004.

[35] M. R. Sontag, J. R. Cunningham, *Clinical application of a CT based treatment planning system,* Comput. Tomogr. 2:117–30, 1978.

[36] L. Beaudoin, *Analytical Approach to the Solution of the Dosimetry in Heterogeneous Media,* M.Sc. Thesis, University of Toronto, 1968.

[37] J. W. Wong, R. M. Henkelman, *A new approach to CT pixel-based photon dose calculations in heterogeneous media*, Med. Phys. 10:199–208,1983.

[38] J. W. Wong, E. D. Slessinger, F. U. Rosenberger, K. Krippner, J. A. Purdy, *The Delta-Volume Method for 3-Dimensional Photon Dose Calculations*, in Proceedings of the 8th

International Conference on the Use of Computers in Radiation Therapy. Toronto, Canada (Silver Spring, MD: Computer Society Press. IEEE) pp. 26–30, 1984.

[39] K. Kappas and J.-C. Rosenwald, *Theoretical and experimental analysis of scatter from inhomogeneous slabs in a 60Co beam: the differential tissue-air ratio method (DTAR)*, Phys. Med. Biol. 31:1211–1228, 1986.

[40] K. Kappas and J.-C. Rosenwald, *A 3-D beam subtraction method for inhomogeneity correction in high energy X-ray radiotherapy*, Radiother. Oncol.5:223–233,1986.

[41] A. L. Boyer, Y. P. Zhu, L. Wang, P. Francois, *Fast Fourier transform convolution calculations of x-ray isodose distributions in homogeneous media*, Med. Phys. 16:248–253, 1989.

[42] T. R. Mackie, J. W. Scrimger, J. J. Battista, *A convolution method of calculating dose for 15-MV x rays*, Med. Phys. 12:188–196, 1985.

[43] R. Mohan, C.-S. Chui, L. Lidofsky, *Differential pencil beam dose computation model for photons*, Med. Phys. 13:64–73, 1986.

[44] A. Ahnesjo, P. Andreo, A. Brahme, *Calculation and application of point spread functions for treatment planning with high energy photon beams*, Acta Oncologica 26:49–56, 1987.

[45] A. Iwasaki, *A method of calculating high-energy photon primary absorbed dose in water using forward and backward spread dose-distribution functions*, Med. Phys. 12:731–7, 1985.

[46] M. K. Woo, J. R. Cunningham, and J. J. Jeziorenski, *Extending the concept of primary and scatter separation to the condition of electronic disequilibrium*, Med. Phys. 17:588–595, 1990.

[47] R. L. Siddon, *Fast calculation of the exact radiological path for a three-dimensional CT array*, Med. Phys. 12:252–255, 1985.

[48] H. Neuenschwander, T. R. Mackie, P. Reckwerdt, *MMC-a high-performance Monte Carlo code for electron beam treatment planning*, Phys. Med. Biol. 40(4):543–74,1995.

[49] M. R. Arnfield, C. Hartmann Siantar, J. Siebers, P. Garmon, L. Cox, R. Mohan, *The impact of electron transport on the accuracy of computed dose*, Med. Phys. 27:1266–1274, 2000.

[50] A. F. Bielajew, D. W. O. Rogers, A. E. Nahum, *The Monte Carlo simulation of ion chamber response to 60Co-resolution of anomalies associated with interfaces*, Phys. Med. Biol. 30(5):419–427, 1985.

[51] Noël G, Antoni D, Barillot I, Chauvet B (2016), *Delineation of organs at risk and dose constraints*, Cancer Radiothérapie. 20, 36-60.

[52] Kharfi F, Ketfi R (2018), *Irradiated black pepper identification based on thermoluminescence of silicate minerals*, Journal of Radioanalytical and Nuclear Chemistry 315, 503–507.

[53] Risø (2015), *Guide to the Risø TL/OSL Reader*, DTU Nutech. Denmark.

[54] Lefkopoulos D, Foulquier JN, Petegnief Y, Touboul E (2001), *Aspects physique et méthodologiques de l'imagerie multimodalité et principe de la planification dosimétrique pour la radiothérapie conformationnelle tridimensionnelle*, Cancer Radiothérapie 5(5), 496-514.

[55] Carrasco P, Jornet N, Duch MA, Weber L, Ginjaume M, Eudaldo T, Jurado D, Ruiz A, Ribas M (2004), *Comparison of dose calculation algorithms in phantoms with lung equivalent heterogeneities under conditions of lateral electronic disequilibrium*, Med Phys31:2, 899–911.

[56] Rana SB (2013), *Dose prediction accuracy of anisotropic analytical algorithm and pencil beam convolution algorithm beyond high density heterogeneity interface*, South Asian J Cancer 2(1), 26–30.

[57] Van Esch A, Tillikainen L, Pyykkonen J, Tenhunen M, Helminen H, Siljamäki S, Alakuijala J, Paiusco M, Lori M, Huyskens DP (2006), *Testing of the analytical anisotropic algorithm for photon dose calculation*, Med Phys.33(11), 4130–4148.

[58] Papanikolaou N, Battista JF, Boyer AL, Kappas C, Klein E, Mackie TE, Sharpe M, Van Dyk J (2004), *AAPM Report No. 85: Tissue Inhomogeneity Corrections for Megavoltage Photon Beams - Report of Task Group No. 65 of the Radiation Therapy Committee of the American Association of Physicists in Medicine*, Madison: Medical Physics Publishing.

[59] Bragg CM, Conway J(2006), *Dosimetric verification of the anisotropic analytical algorithm for radiotherapy treatment planning*, Radiother Oncol 81, 315–323.

[60] Ronde HS, Hoffmann L (2009), *Validation of Varian's AAA algorithm with focus on lung treatments*, Acta Oncol 48, 209–215.

[61] Kry SF, Alvarez P, Molineu A, Amador C, Galvin J, Followil DS (2013), *Algorithms used in heterogenous dose calculations show systematic differences as measured with Radiological Physics Center's anthropomorphic thorax phantom used for RTOG credentialing*, Int. J. RadiatOncolBiol Phys 85(1), 95-100.

[62] Ottosson W, Fehrens CF, Andersen CE(2015), *Dose verification of radiotherapy for lung cancer by using plastic scintillator dosimetry and a heterogeneous phantom,* J Phys: Conf. Ser.573 012022.

[63] McCurdy Boyd MC, McCowan PM (2017), *In vivo dosimetry for lung radiotherapy including SBRT*. PhysicaMedica 44, 123–130.